creative commons

COMMONS DEED

저작자표시-비영리-동일조건변경허락 2.0 대한민국

이용자는 아래의 조건을 따르는 경우에 한하여 자유롭게

- 이 저작물을 복제, 배포, 전송, 전시, 공연 및 방송할 수 있습니다.
- 이차적 저작물을 작성할 수 있습니다.

다음과 같은 조건을 따라야 합니다:

저작자표시. 귀하는 원저작자를 표시하여야 합니다.

비영리. 귀하는 이 저작물을 영리 목적으로 이용할 수 없습니다.

동일조건변경허락. 귀하가 이 저작물을 개작, 변형 또는 가공했을 경우에는, 이 저작물과 동일한 이용허락조건하에서만 배포할 수 있습니다.

- 귀하는, 이 저작물의 재이용이나 배포의 경우, 이 저작물에 적용된 이용허락조건을 명확하게 나타내어야 합니다.
- 저작권자로부터 별도의 허가를 받으면 이러한 조건들은 적용되지 않습니다.

저작권법에 따른 이용자의 권리는 위의 내용에 의하여 영향을 받지 않습니다.

이것은 이용허락규약(Legal Code)을 이해하기 쉽게 요약한 것입니다.

Disclaimer

dCollection

공학박사학위논문

Preparation of Microporous Polymers by Metal-Catalyzed Coupling and Thiol-Yne Addition Reactions of Multifunctional Building Blocks

다기능성 빌딩블록의 금속 촉매반응 및 싸이올-인 반응을 이용한 다공성 고분자의 제조에 관한 연구

2013년 8월

서울대학교 대학원

재료공학부

이 현 표

Preparation of Microporous Polymers by Metal-Catalyzed Coupling and Thiol-Yne Addition Reactions of Multifunctional Building Blocks

다기능성 빌딩블록의 금속 촉매반응 및 싸이올-인 반응을 이용한 다공성 고분자의 제조에 관한 연구

지도교수 장 지 영

이 논문을 공학박사 학위논문으로 제출함
2013년 4월

서울대학교 대학원
재료공학부
이 현 표

이현표의 공학박사 학위논문을 인준함
2013년 7월

위 원 장 조 원 호 (인)
부위원장 장 지 영 (인)
위 원 박 종 래 (인)
위 원 안 철 희 (인)
위 원 임 순 호 (인)

Abstract

Preparation of Microporous Polymers by Metal-Catalyzed Coupling and Thiol-Yne Addition Reactions of Multifunctional Building Blocks

Hyunpyo Lee

Department of Materials Science and Engineering

Seoul National University

Microporous organic polymers with high surface areas and physicochemical stability have potential applications in gas storage, catalysis, and separation. In this study, various microporous polymers were prepared by thiol-yne addition reaction and metal-catalyzed carbon-carbon bond forming reactions of multifunctional organic compounds.

A microporous polymer was synthesized by thiol-yne addition reaction of tetrakis(4-ethynylphenyl)adamantane and benzene-1,3,5-trithiol in the presence of AIBN. Au nanoparticles (Au NPs) were prepared by $NaBH_4$ reduction reaction of $HAuCl_4$ and immobilized in the polymer network via an interaction with sulfur groups. The BET surface area of the microporous polymer was 576 m^2/g and decreased to 104 m^2/g after incorporation of the Au NPs. The Au NPs loaded microporous polymer showed a catalytic activity in hydrogenation

reaction of 4-nitrophenol.

A bisphenol-A imprinted microporous polymer was prepared by Yamamoto cross-coupling reaction of tetrakis(4-bromophenyl)methane and a bromophenyl-bisphenol-A (template) complex. After the extraction of the template molecules, the BET surface area of the polymer increased from 25.3 m^2/g to 562 m^2/g. The specific recognition ability of the polymer to bisphenol-A and its structural analogues was investigated by HPLC analysis. The imprinted polymer showed a high rebinding ability of bisphenol-A compared with that of non-imprinted polymer. In kinetic study, a 90 % of an equilibrium amount was recognized within 5 min after the addition of bisphenol-A.

Microporous polymers, TPE-DB, TPE-TB, and TPE-AD were prepared by Sonogashira-Hagihara cross-coupling reaction of tetrakis(4-iodophenyl)ethane (TIPE) with 1,4-diethynylbenzene (DB), 1,3,5-triethynylbenzene (TB), and tetrakis(4-ethynylphenyl)adamantane (AD), respectively. Polymers, TPE-DB/TB(1:2) and TPE-DB/TB(3:2), having two different ethynyl units were also obtained by using mixtures of 1,4-diethynylbenzene and 1,3,5-triethynylbenzene in molar ratios of 1 : 2 and 3 : 2, respectively, for the coupling reaction. Among the polymers with the one type of ethynyl units, TPE-TB showed the highest BET surface area of 1230 m^2/g, followed by TPE-DB (405 m^2/g) and TPE-AD (615 m^2/g). TPE-DB/TB(3:2) with two different

ethynyl units exhibited a significantly enhanced BET surface area of 1840 m^2/g compared with TPE-DB and TPE-TB. The polymers except TPE-DB showed CO_2 and H_2 uptakes over 40 and 100 cm^3/g, respectively.

Microporous polymers were obtained by Heck cross-coupling reaction of 1,3,5-trichlorobenzene or 1,3,5-tri(4-bromophenyl)benzene with divinylbenzene. The PCP pincer complex was synthesized from $Pd(COD)Cl_2$ and C_6H_4-2,6-$(OP^iPr_2)_2$ and used as a catalyst for the reaction. After carbonization, the volume fraction of micropores with a diameter less than 1 nm increased and the polymers showed the enhanced CO_2 and H_2 uptakes.

Keywords: microporous material, gas storage, catalysis, imprinted polymer.

Student Number: 2006-20875

Contents

Abstract i
Contents iv
List of Schemes vi
List of Tables viii
List of Figures ix
Chapter I. Introduction 1
I-1. Introduction to Microporous Materials 2
I-2. Preparation Methods of MOPs 5
I-2.1. Condensation Reaction 5
I-2.2. Cyclotrimerization 10
I-2.3. Yamamoto Cross-Coupling Reaction 14
I-2.4. Sonogashira-Hagihara Cross-Coupling Reaction 16
I-2.5. Suzuki-Miyaura Cross-Coupling Reaction 19
I-2.6. Friedel-Crafts Reaction 20
I-3. Applications of Microporous Organic Polymers 22
Chapter II. Preparation of Au Nanoparticles Inside a Microporous Organic Polymer Obtained by Thiol-Yne Addition Reaction and Their Catalytic Activity 26
II-1. Introduction 27
II-2. Experimental 29
II-3. Results and Discussion 34
II-4 Conclusion 47
Chapter III. Preparation of Molecularly Imprinted Microporous Polymers by Yamamoto Cross-Coupling Reaction 48
III-1. Introduction 49

III-2. Experimental 51
III-3. Results and Discussion 55
III-4. Conclusion 67
Chapter IV. Preparation of Microporous Polymers Consisting of Tetraphenylethene and Alkyne Units 68
IV-1. Introduction 69
IV-2. Experimental 71
IV-3. Results and Discussion 75
IV-4. Conclusion 91
Chapter V. Preparation of Microporous Polymers by Heck Cross-Coupling Reaction with a PCP Pincer Catalyst 92
V-1. Introduction 93
V-2. Experimental 94
V-3. Results and Discussion 98
V-4 Conclusion 107
Chapter VI. References 108
국문요약 122

List of Schemes

Scheme I-1. Synthesis of COF-1.

Scheme I-2. Synthesis of COF-42 and 43 by imine condensation reaction.

Scheme I-3. Synthesis of 3D COF-300.

Scheme I-4. Synthesis of CTF-1.

Scheme I-5. Cyclotrimerization of cyanate functional groups and synthesis of porous cyanate resin.

Scheme I-6. Synthesis of $Ti(O^iPr)_4$ treated CCP.

Scheme I-7. Synthesis of Ru- and Ir-incorporating PCPs.

Scheme I-8. Synthesis of PAF-1.

Scheme I-9. Synthesis of PPN-4.

Scheme I-10. Reaction mechanism of Sonogashira-Hagihara cross-coupling reaction.

Scheme I-11. Synthesis of CMPs.

Scheme I-12. Synthesis of PP-CMP.

Scheme I-13. Synthesis of a microporous polymer by Friedel-Crafts reaction.

Scheme I-14. Synthesis of FeP-CMP and catalytic oxidation of thioanisole by FeP-CMP.

Scheme II-1. Synthesis of tetrakis(4-ethynylphenyl)adamantane.

Scheme II-2. Preparation of the microporous polymer.

Scheme II-3. Schematic description for the model reaction with thiophenol and phenylacetylene.

Scheme II-4. Preparation of the Au NPs loaded microporous polymer.

Scheme III-1. Synthesis of BisA-Br.

Scheme III-2. Synthesis of the imprinted microporous polymer.

Scheme IV-1. Synthesis of microporous polymers TPE-DB, TPE-TB, and TPE-AD.

Scheme IV-2. Synthesis of microporous polymers TPE-DB/TB(1:2) and TPE-DB/TB(3:2) having two different ethynyl units.

Scheme V-1. Synthesis of the PCP catalyst.

Scheme V-2. Preparation of MP-H1 and MP-H2.

List of Tables

Table IV-1. Porosity Properties and Gas Uptake Capacities of the Microporous Polymers.

List of Figures

Figure II-1. Solid state ^{13}C NMR spectrum of the microporous polymer.

Figure II-2. FT-IR spectra of the microporous polymer and the Au loaded microporous polymer.

Figure II-3. ^{1}H NMR spectra of a solution of thiophenol and phenylacetylene in DMSO-d_6 measured (a) before heating without AIBN, (b) after heating with AIBN for 3 h and (c) 24 h.

Figure II-4. SEM image and WXRD pattern of the microporous polymer.

Figure II-5. (a) Nitrogen adsorption-desorption isotherms at 77 K and (b) NLDFT pore size distribution of the Au NPs loaded microporous polymer and the microporous polymer.

Figure II-6. HR-TEM image of Au NPs loaded microporous polymer.

Figure II-7. Powder XRD pattern of Au NPs loaded microporous polymer.

Figure II-8. X-ray photoelectron spectrum of the Au NPs loaded microporous polymer and high-resolution X-ray Photoelectron spectrum (inset).

Figure II-9. Uv-vis spectra measured during the catalytic reduction of 4-nitrophenol into 4-aminophenol in the presence of the Au NPs loaded microporous polymer.

Figure III-1. ^{13}C CP/MAS NMR spectra of the imprinted microporous polymer before and after extraction. The asterisk marks a rotational sideband.

Figure III-2. SEM images of (a) the microporous polymer before extraction and (b) after extraction, and (c) the non-imprinted microporous polymer.

Figure III-3. TEM images of (a) the microporous polymer before extraction and (b) after extraction.

Figure III-4. Wide angle X-ray diffraction patterns of the the microporous polymer before and after extraction.

Figure III-5. DSC thermograms of the microporous polymer before and after extraction.

Figure III-6. (a) N_2 adsorption-desorption isotherms at 77 K and (b) NLDFT pore size distributions of the microporous polymer before and after extraction.

Figure III-7. Binding selectivity of the imprinted microporous polymer and the control polymer.

Figure III-8. Binding selectivity of the imprinted microporous polymer and the control polymer.

Figure III-8. Kinetic binding profiles of bisphenol-A to the imprinted microporous polymer and the control polymer.

Figure IV-1. ^{13}C CP/MAS NMR spectra of (a) TPE-DB, (b) TPE-TB, (c) TPE-AD, (d) TPE-DB/TB(1:2), and (e)TPE-DB/TB(3:2). The asterisk marks a rotational sideband.

Figure IV-2. SEM images of (a) TPE-DB, (b) TPE-TB, (c) TPE-AD, (d) TPE-DB/TB(1:2), and (e) TPE-DB/TB(3:2).

Figure IV-3. WXRD patterns of the polymers: (a) TPE-DB, TPE-TB, and TPE-AD; (b) TPE-DB/TB(1:2) and TPE-DB/TB(3:2).

Figure IV-4. (a) Nitrogen adsorption-desorption isotherms and (b) NLDFT pore size distributions of TPE-DB, TPE-TB, and TPE-AD.

Figure IV-5. (a) Nitrogen adsorption-desorption isotherms and (b) NLDFT pore size distributions of TPE-DB/TB(1:2) and TPE-DB/TB(3:2).

Figure IV-6. (a) CO_2 (273 K) and (b) H_2 (77 K) uptake behaviors of the polymers.

Figure V-1. SEM images of (a) MP-H1 and (b) MP-H2.

Figure V-2. ^{13}C CP/MAS NMR spectra of MP-H1 and MP-H2.

Figure V-3. N_2 adsorption-desorption isotherms of MP-H1 and MP-H2 at 77K.

Figure V-4. (a) N_2 adsorption-desorption isotherms at 77 K and (b) NLDFT pore size distribution of MP-H2C.

Figure V-5. CO_2 adsorption isotherms of MP-H2C at 273 and 298 K.

Figure V-6. CO_2 heat of adsorption of MP-H2C.

Figure V-7. H_2 uptake of MP-H2C.

Chapter I. Introduction

I-1. Introduction to Microporous Materials

A porous material is a material containing pores that are classified into several types by their diameters. According to the IUPAC notation,[1] microporous materials have pore diameters less than 2 nm. Mesoporous materials have pore diameters greater than 2 nm, but less than 50 nm. Macroporous materials have pore diameters greater than 50 nm.

The porosity of microporous materials is measured by gas adsorption-desorption isotherm. Langmuir and Brunauer-Emmett-Teller (BET) surface area analysis are used to determine the surface areas of microporous materials. The Langmuir surface area is based on the monolayer coverage of the surface by the adsorbates.[2] The BET surface area is calculated by a model of adsorption which incorporates multilayer coverage.[3] The BET surface area is most commonly reported because the BET theory accommodates multilayer adsorption. Microporous materials usually show high BET and Langmuir surface areas because micropores in the materials contribute to the adsorption of adsorbate gas molecules.

The pore size distribution of the porous materials can be determined by several methods such as Horvath-Kawazoe (HK), Barrett-Joyner-Halenda (BJH), and non-local density functional theory (NLDFT). The HK method

provides a way for micropore volume distribution by size that is extracted from the experimental isotherm.[4] The original H-K method is based on slit-shaped pores. However, Saito-Foley[5,6] and Cheng-Yang[7] extend this method in order to apply to cylindrical and spherical pores, respectively. The HK method is restricted to the micropore region. The BJH method determines the pore size for the mesopore and small macropore from the Kelvin equation and the selected statistical thickness (t-curve) equation.[8] The NLDFT pore size distribution provides a microscopic treatment of sorption phenomena in micro-and mesopores on a molecular level based on statistical mechanics.[9-11] A complex mathematical modeling of gas-solid and gas-gas (gas-liquid) interactions with geometrical considerations (pore geometry) leads to realistic density profiles for the confined fluid as a function of temperature and pressure.

Typical microporous materials are zeolite, activated carbon, MOFs (Metal Organic Frameworks),[12-20] and MOPs (Microporous Organic Polymers). MOPs consist of light elements such as C, H, B, N and O and therefore have very low densities compared with other microporous materials. Various types of porous organic polymers have been reported, each with their own structural characteristics described as COFs (Covalent Organic Frameworks),[21-29] PIM (Polymers of Intrinsic Microporosity),[30-32] HCPs (Hyper Cross-linked Polymers),[33,34] CMPs (Conjugated Microporous Polymers),[35-46] PAFs (Porous

Aromatic Frameworks),[47] etc.

I-2. Preparation Methods of MOPs

There are available a wide range of synthetic methods for preparing MOPs, including condensation, cyclotrimerization, Yamamoto cross-coupling, Sonogashira-Hagihara cross-coupling, Suzuki-Miyuara cross-coupling, and Friedel-craft reaction.

I-2.1. Condensation Reaction

Condensation reactions are very useful reaction for preparing the microporous polymers by connection of the multifunctional organic linkers. Self-condensation reaction of three boronic acid groups formed the six-membered rings by connecting the organic linkers with C-B covalent bonds under solvothermal conditions to produce COFs.[21-29] The COFs are crystalline materials due to the reversible formation of strong B-O bonds in solvothermal condition. Yaghi and his coworkers reported COF-1 by self-condensation reaction of benzene-1,4-diboronic acid in solvothermal condition [Scheme I-1]. The BET surface area of COF-1 was 711 m^2/g. The condensation reactions of tetrahedral tetra(4-dihydroxyborylphenyl)methane (TBPM) or silane analog (TBPS) with triangular 2,3,6,7,10,11-hexahydroxytriphenylene (HHTP)

provided crystalline 3D COFs, COF-102 and COF-103, repectively. 3D COF-103 showed a high BET surface area of 4,210 m^2/g.

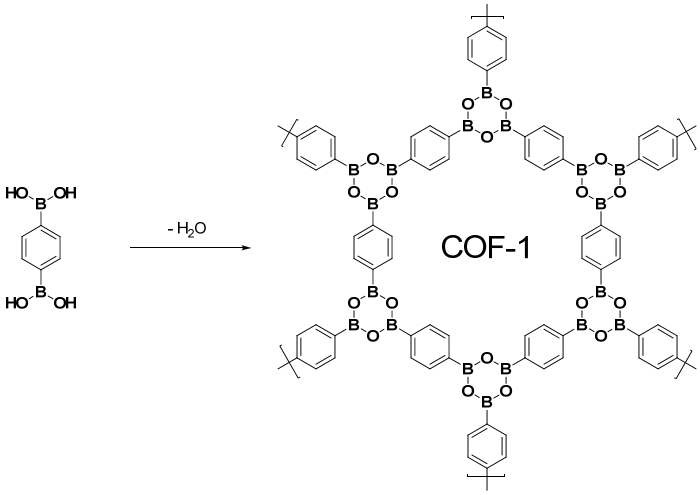

Scheme I-1. Synthesis of COF-1.

An imine condensation reaction between an aldehyde and an amine has been used for preparing microporous polymers.[48-51] The mechanism leading to the Schiff base involves a number of steps that are reversible. Müllen and his coworkers reported melamine-based microporous polymers obtained from dialdehyde and trialdehyde monomers.[48] The microporous polymers had BET surface areas of 800 – 1300 m^2/g. The high nitrogen contents over 40 wt.% was considered to be useful for the storage of CO_2 and the development of novel proton conducting materials.

COF-42 and COF-43 were synthesized by the imine condensation reaction of 2,5-diethoxyterephthalohydrazide and 1,3,5-triformylbenzene, or 1,3,5-tris(4-formylphenyl)benzene, in solvothermal conditions [Figure I-2].[49] The crystallinity of COF-42 and COF-43 was controlled by the pH-dependent reversibility of hydrazone linkages. Unlike COF-42 and 43, the condensation of the tetrahedral building block tetrakis(4-aminophenyl)methane with the linear linking unit terephthaldehyde produced a material with an extended 3-D framework structure (COF-300) [Figure I-3].[50] The COF-300 had a BET surface area of 1360 m^2/g with a pore size of 7.2 Å.

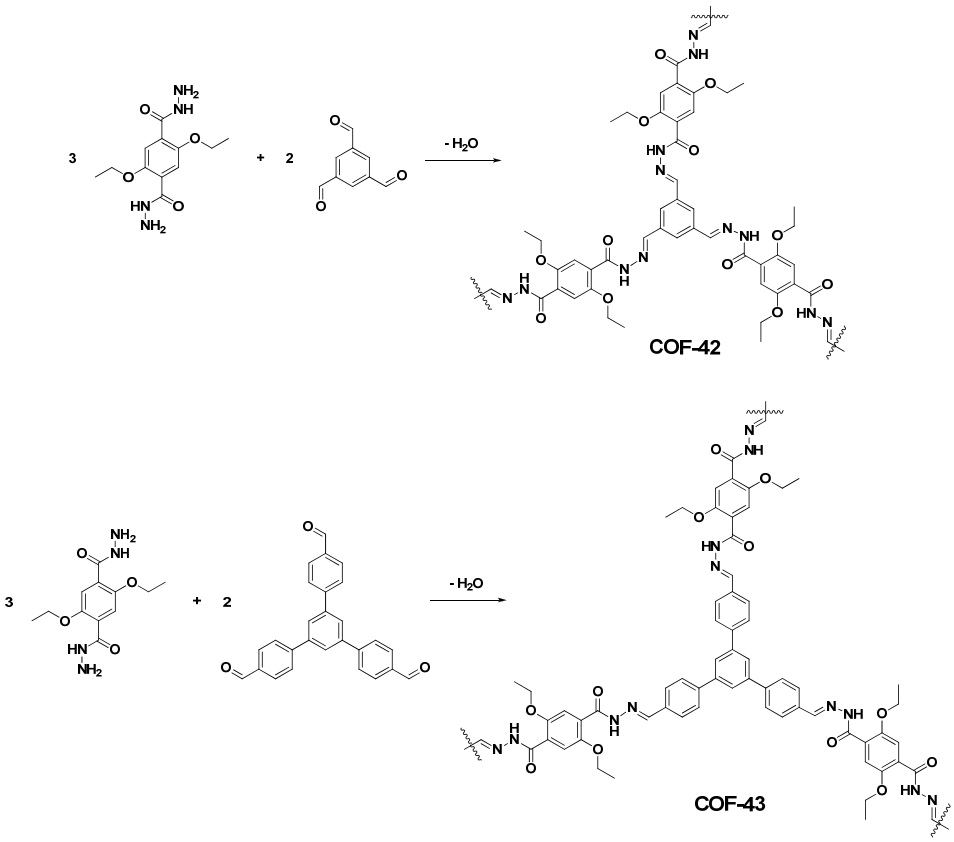

Scheme I-2. Synthesis of COF-42 and COF-43 by imine-condensation reaction.

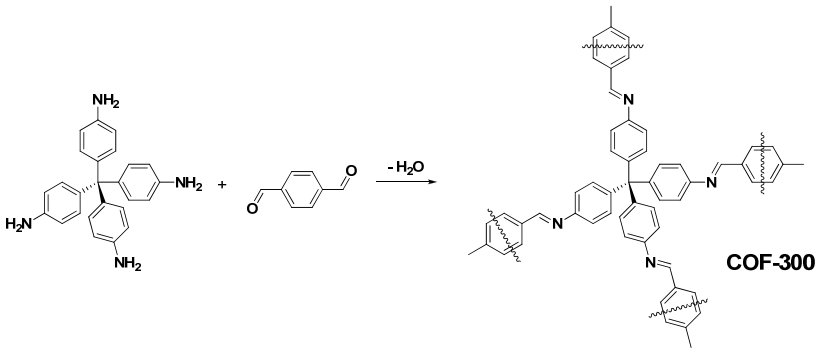

Scheme I-3. Synthesis of 3D COF-300.

A benzimidazole-linked polymer (BILP-1) was prepared by the condensation reaction between 2,3,6,7,10,11-hexaaminotriphenylene (HATP) and tetrakis(4-formylphenyl) methane (TFPM).[52] BILP-1 had an amine group on the surface which could interact with CO_2 and showed a relatively high CO_2 uptake.

Polyimide networks were prepared by condensation reaction of tetrahedral-amine monomers, for example, 2,2′,7,7′-tetraamino-9,9′-spirobifluorene and tetrakis(4-aminophenyl)methane with dianhydride functional monomers.[53-55] The BET surface areas of the polyimide networks were below 1,200 m^2/g. These networks had several advantages such as inexpensive, thermally stable and chemically stable due to their chemical structure.

I-2.2. Cyclotrimerization

Triazine rings can be produced by a cyclotrimerization reaction of three nitrile functional groups in the ionothermal conditions. The cyclotrimerization reaction of the building blocks having two nitrile functional groups at the end was used to prepare CTFs (Covalent Triazine-based Frameworks) by formation of triazine rings in the presence of $ZnCl_2$ at high temperatures.[56-59] The CTF-1 had a high BET surface area of 1120 m^2/g and showed a crystalline structure with hexagonal packing of pores. Scheme I-4 represents the synthetic procedures of CTF-1.

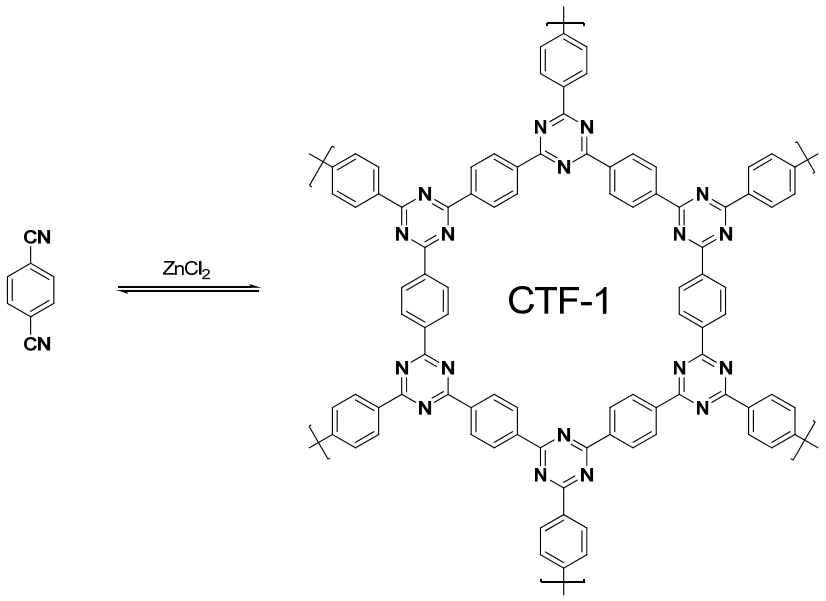

Scheme I-4. Synthesis of CTF-1.

Cyanate groups also undergo thermal cyclotrimerization to produce triazine rings connected by aryl ether linkages [Scheme I-5].[60] Porous cyanate resins were prepared by a cyclotrimerization reaction of cyanate monomers with tetrahedral and triangular shapes such as tetrakis(4-cyanatophenyl)silane, tetrakis(4-cyanatobiphenyl)silane, and tris(4-cyanatobiphenyl)amine [Scheme I-5]. The BET surface area of porous cyanate resins were 540-960 m^2/g.

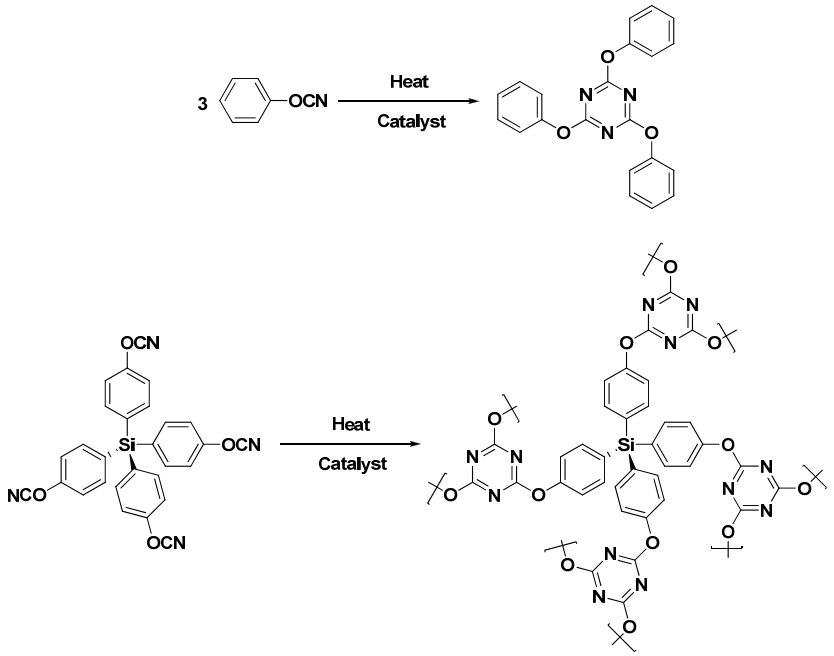

Scheme I-5. Cyclotrimerization of cyanate functional groups and synthesis of porous cyanate resin.

Lin and his coworkers synthesized the chiral cross-linked polymers by a Co-mediated trimerization reaction with 1,1'-binaphthyl building blocks [Scheme I-6].[61] The reaction was carried out using $Co_2(CO)_8$ as a catalyst. The treatment of chiral dihydroxyl-containing CCPs (Chiral Cross-linked Polymers) with $Ti(O^iPr)_4$ produced the highly active Lewis acid catalysts.

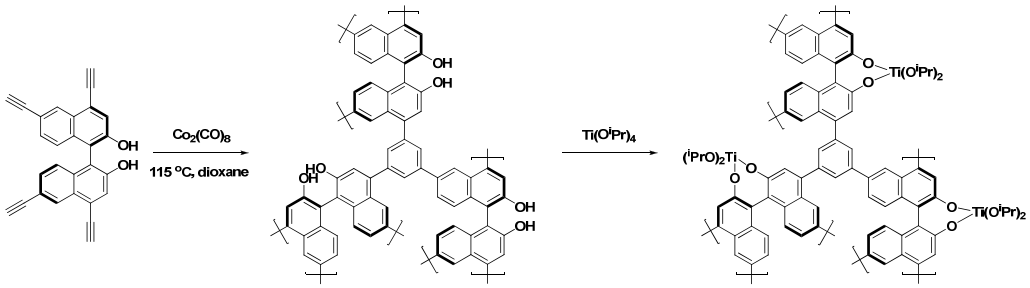

Scheme I-6. Synthesis of $Ti(O^iPr)_4$ incorporated CCP.

The same group also reported Ru- and Ir-incorporating porous cross-linked polymers (PCPs)[62] that were prepared by copolymerizing $[(ppy)_2Ir(debpy)]Cl$ and $[(bpy)_2Ru(debpy)]Cl_2$ (bpy = 2,2′-bipyridine, ppy = 2-phenylpyridine, debpy = 5,5′-diethynyl-2,2′-bipyridine) with tetrakis(4-ethynylphenyl)methane [Scheme I-7]. Ir-PCP and Ru-PCP had BET surface areas of 1550 and 1350 m^2/g, respectively.

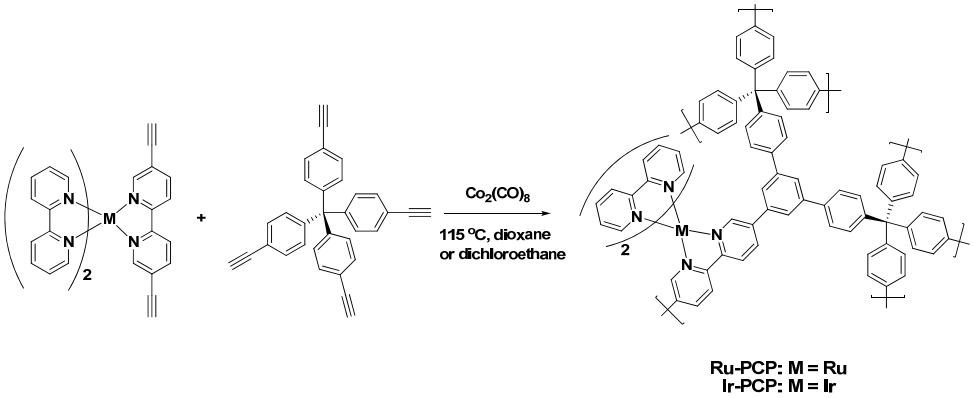

Scheme I-7. Synthesis of Ru- and Ir-incorporating PCPs.

I-2.3. Yamamoto Cross-Coupling Reaction

Yamamoto cross-coupling reaction requires equimolar quantities of Ni(0) complexes as a catalyst because Ni(0) can't be regenerated during the reaction pathway.[63] This Ni(0) catalyzed homo-coupling of aryl halides is a very efficient approach to the synthesis of biaryls or heterobiaryls. The mechanism of Yamamoto cross-coupling reaction consists of three steps: (1) oxidative addition of Ar-X to Ni(0) $(COD)_2$ to form Ni(II)ArX-$(COD)_2$ and (2) further oxidative addition of Ar-X to form Ni(IV)Ar_2X_2, followed by (3) reductive elimination to generate biaryl and Ni(II)X_2.

Zhu and his coworkers prepared a porous aromatic framework (PAF)-1 via Yamamoto cross-coupling reaction of tetrakis(4-bromophenyl)methane [Figure I-8].[47] The PAF-1 had a tetrahedral structure like a diamond, and showed outstanding gas uptake properties. Its BET surface area and Langmuir surface area were 5,600 and 7,100 m^2/g, respectively. PAF-1 also had high thermal and chemical stability, which showed the possibility that amorphous porous organic polymers could replace MOF.

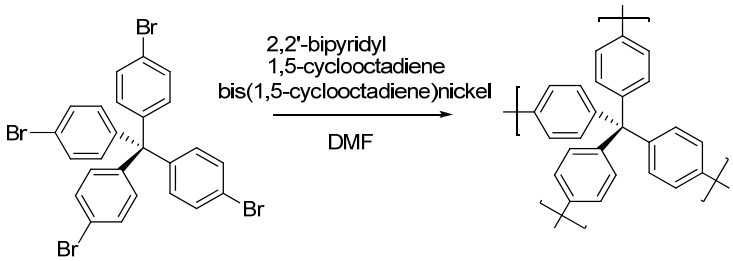

Scheme I-8. Synthesis of PAF-1.

Zhou and his coworkers prepared porous polymer networks (PPNs) by Yamamoto cross-coupling reaction with tetrahedral monomers [Figure I-9].[64] PPN-4 prepared with tetrakis(4-bromophenyl)silane showed BET and Langmuir surface areas of 6,460 and 10,000 m^2/g, respectively.

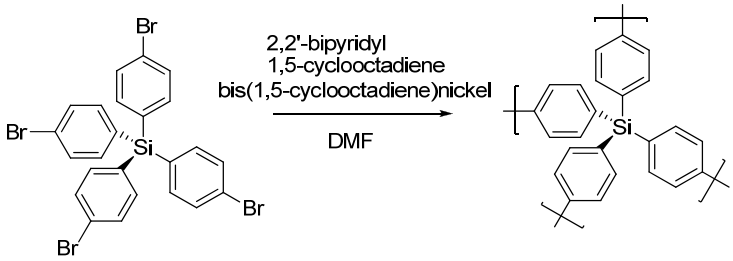

Scheme I-9. Synthesis of PPN-4.

I-2.4. Sonogashira-Hagihara Cross-Coupling Reaction

Direct introduction of sp^2 carbon to alkynes by the reaction of Cu acetylides with aryl and alkenyl halides to form arylalkynes and alkenylalkynes is known as the Castro reaction. Later it was found that the coupling of terminal alkynes (1-alkynes) with halides proceeds more smoothly by using Pd catalysts. In 1975 Sonogashira and Hagihara found that the addition of CuI as a co-catalyst gave better results, and the Pd(0)-CuI-catalyzed reaction is called as Sonogashira-Hagihara reaction.[65,66]

The reaction is explained by the following mechanism [Scheme I-10]. At first, CuI activates 1-alkynes by forming the Cu acetylides, which undergo transmetallation with arylpalladium halides to form the alkynylarylpalladium species, and reductive elimination is the final step.

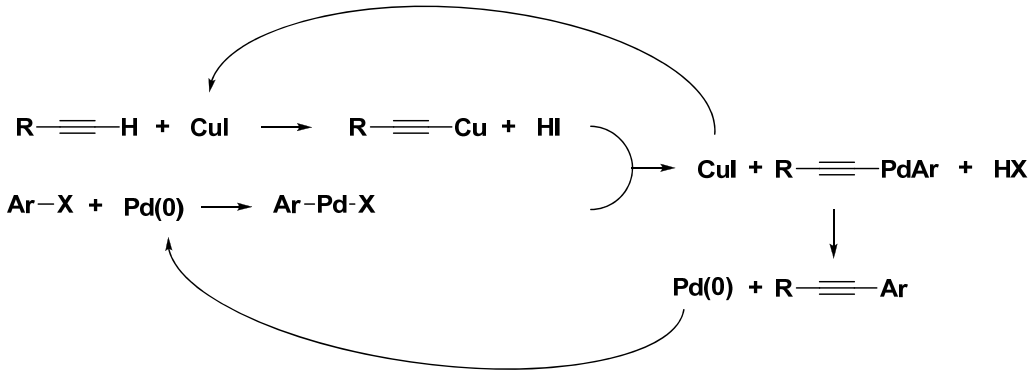

Scheme I-10. Reaction mechanism of Sonogashira-Hagihara cross-coupling reaction.

Sonogashira-Hagihara cross-coupling reaction has been used to prepare conjugated microporous polymers (CMPs). Sonogashira-Hagihara cross-coupling reaction connects acetylene group and aromatic ring via a covalent bond. Cooper and his coworkers prepared CMP-1 with 1,3,5-triethynylbenzene and 1,4-diiodobenzene.[35] The CMPs had a relatively low surface area of below 1,000 m^2/g.[41,67,68] CMPs could be functionalized with various pendant groups such as amine, fluorine, nitro, and pyridyl group.

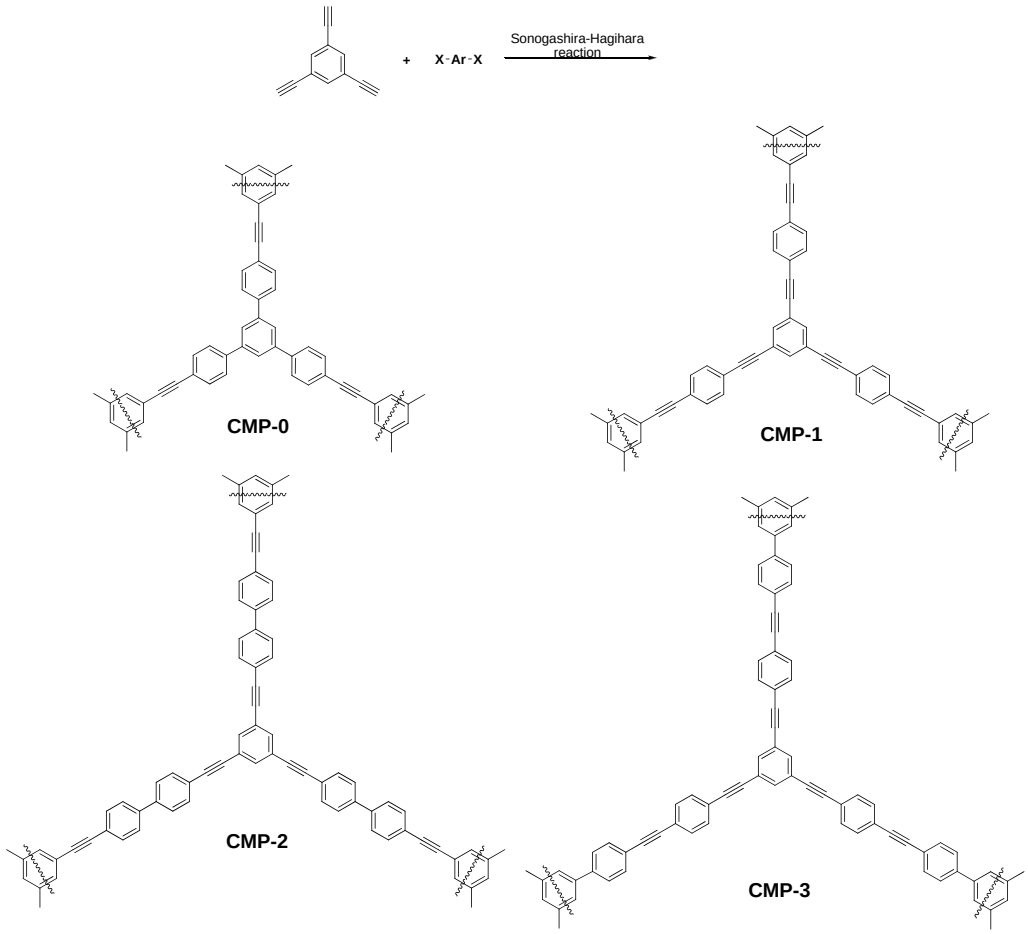

Scheme I-11. Synthesis of CMPs.

I-2.5. Suzuki-Miyaura Cross-Coupling Reaction

Suzuki-Miyaura cross-coupling reaction is a coupling reaction between organoboron and organohalide compounds.[69] Due to the low nucleophilicity of organic groups R on the B atom, their transmetallation is difficult. The coupling reaction proceeds via transmetallation in the presence of bases. Suzuki-Miyaura coupling reaction is very popular among Pd-catalyzed cross-couplings on account of several advantages: (1) commercial availability of a large number of organoboranes especially boronic acids and their esters, (2) stability of boronic acids to heat, air, and moisture, (3) tolerance to a broad range of functional groups, (4) mild reaction conditions, and (5) easy separation of inorganic boron from reaction mixture.

Jiang and his coworkers prepared PP-CMP by the Suzuki-Miyaura coupling reaction of 1,2,4,5-tetrabromobenzene and 1,4-benzene diboronic acid as building blocks [Scheme I-12].[70] After incorporating coumarin-6 molecules into the PP-CMP, PP-CMP was capable of excitation energy migration over a conjugated framework. Coumarin6@PP-CMP harvested a wide range of photons from the ultraviolet to visible regions and converted them to brilliant green luminescence.

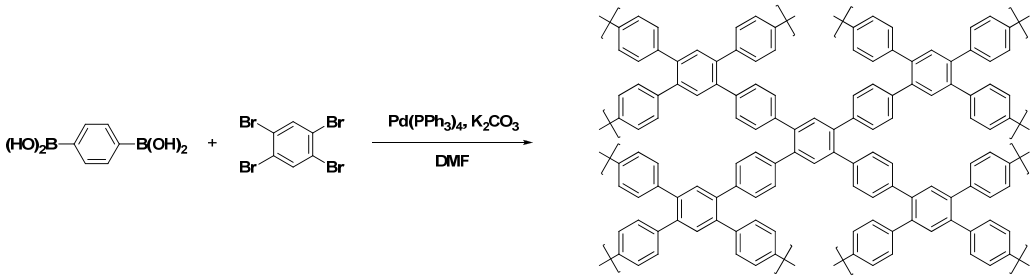

Scheme I-12. Synthesis of PP-CMP.

I-2.6. Friedel-Crafts Reaction

Tan and his coworkers prepared nanoporous polymer networks using a one-step Friedel-Crafts reaction with aromatic and heterocyclic cores [Scheme I-13].[71,72] Formaldehyde dimethyl acetal was used as a cross-linker and various aromatic and heterocyclic cores reacted with formaldehyde dimethyl acetal to form highly cross-linked microporous polymers. This method had several advantages such as versatility, large-scale production, and functionalization with different structural building blocks. In the case of pyrrole core, the gas selectivity of CO_2 over N_2 had an extraordinarily high value (about 117 at 273 K).

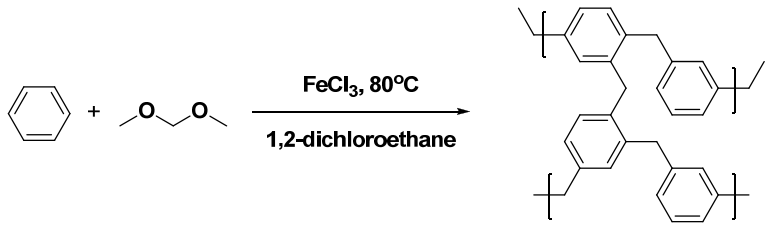

Scheme I-13. Synthesis of a microporous polymer by Friedel-Crafts reaction.

Kaskel and coworkers synthesized microporous polymers by Friedel-Crafts reaction of 4,4'-bis(chloromethyl)biphenyl (BCMBP) with fluorene (FLUO), 9,9'-spirobi(fluorene) (sFLUO), dibenzofuran (DBF) and dibenzothiophene (DBT).[73] Adams and his coworker also prepared a microporous polymer by Friedel-Crafts reaction of formaldehyde dimethyl acetal with various ratios of benzene and aniline.[74]

I-3. Applications of Microporous Organic Polymers

Microporous organic polymers have potential applications in gas storage, separation, and catalysis. Hydrogen has been proposed as an emerging energy source by being able to replace traditional fossil fuels due to its single and clean combustion by product and its chemical energy density (142 MJ/kg).[75] There are essentially three ways to store hydrogen. Storing the gas in a simple tank is attractively simple, but storing reasonable amounts per volume requires liquefaction at very low temperatures and/or high pressures. Storing the hydrogen as a chemical compound such as a metal or nonmetal hydride is an option, but the large energy change between the stored and the released hydrogen leads to many complications in reversibility, kinetics, and heat management issues. The third alternative is to use physisorption on a microporous material. Zeolites,[76] MOFs,[77] and carbon materials[78,79] have all been extensively studied for their hydrogen adsorption properties and organic polymers are of increasing interest.[80]

3D microporous polymers have been anticipated to have substantial potential for gas storage due to their extremely high surface areas and low densities. There have been a number of reports both on their predicted and measured gas uptakes.[81,82]

The combustion of fossil fuel increased the concentration of CO_2 in the atmosphere which is thought to be a major contributor to global warming. CO_2 capture and storage is thus currently a very active research area.

The capture of CO_2 has been studied using a variety of materials. Amine solvents have been used for CO_2 capture by a chemical interaction with CO_2 molecules. However, the recycling of amine solvents by heating leads to a large energy penalty.

A variety of microporous organic polymers have been studied for the adsorption of CO_2. For CO_2 capture and selective separation, MOPs must have strong interaction, high surface area, and favorable pore size. Recently, BILP-1 (Benzimidazole-Linked Polymer) denoted a relatively high surface area (1,170 m^2/g) and high CO_2 uptake capacity (188 mg/g, 273 K, 1 bar).[52] Selectivity is significant for gas separation. In particular, a low pressure adsorption is important to separate CO_2 from the post-combustion gas. The selectivity of CO_2 over N_2 of BILP-1 was 70 at 273 K, which surpassed those of carbon based materials or ZIFs

The use of microporous organic polymers for heterogeneous catalysts has been studied considerably because of their advantages such as good chemical and physical stability, synthetic diversity, and potential for pore size control. There are two main strategies for introduction of catalytic moieties into MOPs.

The first is the bottom-up approach by which the building blocks with catalytic function groups are applied directly to construct the polymer networks. This allows the catalytically active sites to be embedded onto the pore wall. The second strategy is to incorporate metal nanocrystals into MOPs via post treatment method.

Iron(III) porphyrin-based CMP (FeP-CMP) with large surface areas and nanometer-scale pores was prepared by the Suzuki cross coupling reaction of an iron(III) tetrakis(4-bromophenyl)porphyrin derivative and 1,4-phenyldiboronic acid in the presence of Pd(0) as a catalyst under alkaline conditions [Scheme I-14].[42,83] FeP-CMP acted as a heterogeneous catalyst for the oxidation of thioanisole to the sulfoxide with selectivities of up to 99 %, conversions of 98 % and turnover numbers of up to 980.

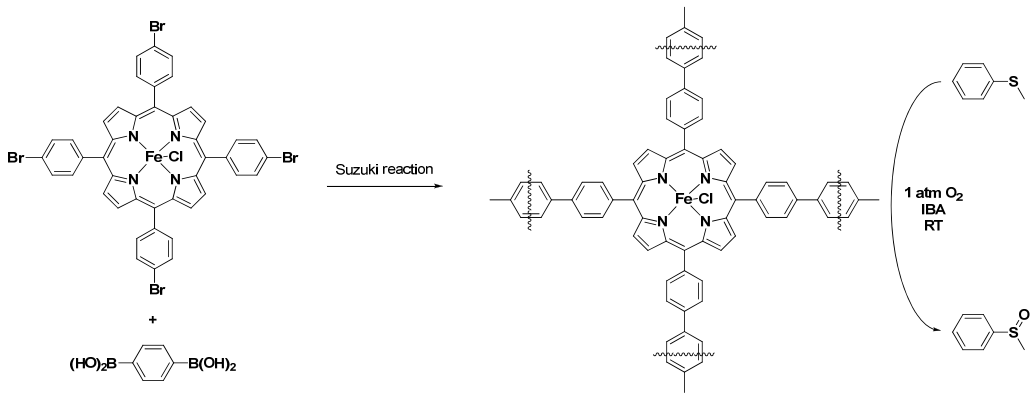

Scheme I-14. Synthesis of FeP-CMP and catalytic oxidation of thioanisole by FeP-CMP.

DMAP (4-dimethylaminopyridine) containing microporous polymer was prepared by Sonogashira–Hagihara cross-coupling reaction of the functional monomer,[84] 3,5-dibromo-N,N-dimethylpyridin-4-amine and 1,3,5-triethynylbenzene. A variety of aliphatic alcohols and phenols could be effectively converted into the corresponding ester products in excellent yields (92–99%).

A metal-organic conjugated microporous polymer (MO-CMP) was prepared by the post treating of a bipyridine-functionalized CMP precursor with a metal complex or by Sonogashira cross-coupling reaction of 1,3,5-triethylbenzene or 1,4-dibromobenzene and a halogenated metal–organic co-monomer.[44] The CMP containing Ir complexes showed catalytic acitivity for reductive amination.

Chapter II. Preparation of Au Nanoparticles Inside a Microporous Organic Polymer Obtained by Thiol-Yne Addition Reaction and Their Catalytic Activity

II-1. Introduction

The thiol-yne reaction between a thiol and an alkyne is an interesting metal catalyst free coupling reaction.[85-87] The reaction proceeds in a high yield via a radical mechanism with the aid of a radical initiator or UV light. A number of multibranched polymers such as dendrimers,[88,89] hyperbranched polymers,[90-92] and star polymers[93] have been synthesized by this reaction. The thiol-yne reaction could be very useful for the synthesis of a highly crosslinked polymer network. The mechanism study of the thyol-yne photopolymerization by Fairbanks et al. showed that each ethynyl group reacted with two thiol groups[94] because the reaction of a thiyl radical with an alkyne group produced a vinyl unit, which was still reactive against another thiyl radical.

In this study, microporous organic polymer was prepared with sulfide and thiol groups by the thiol-yne reaction of a tetraethynyl compound with a trithiol. Gold nanoparticles were incorporated into the MOP by in-situ reduction reaction of $HAuCl_4$ with $NaBH_4$. It was expected that the sulfide and thiol groups would prevent the aggregation of the gold nanoparticles by interacting with their surfaces. Au nanoparticles (Au NPs) attracted considerable attention for their catalytic activities in organic reaction such as reduction with borohydride,[95-99] oxidation of alcohols,[100,101] and CO.[102,103] Au NPs in the

microporous polymer were used as a catalyst for amination reaction of 4-nitrophenol in the presence of $NaBH_4$.

II-2. Experimental

Materials. 1-Bromoadamantane, triethylamine, $AlCl_3$, trimethylsilylacetylene, $NaBH_4$, 4-nitrophenol, K_2CO_3, thiophenol, CuI, dichlorobis(triphenylphosphine)palladium(II), phenylacetylene and gold chloride hydrate ($HAuCl_4$) were purchased from Aldrich and used as received. Azobisisobutyronitrile (AIBN) was purchased from Aldrich and recrystallized in methanol before use. 1,3,5-Benzenetrithiol and iodine was purchased from TCI and used as received. Other reagent-grade solvents were used as received.

Measurements. ^{1}H Nuclear magnetic resonance was carried out on a Bruker Avance-300 (300 MHz). ^{13}C Solid state NMR measurements were carried out on a Bruker 400 Solid/Micro-Imaging High Resolution NMR (100 MHz). N_2 and CO_2 uptake amounts were measured by using a Belsorp-Max (BEL Japan, Inc.) apparatus. Fourier transform infrared (FT-IR) measurements were recorded on a PERKIN ELMER Spectrum GX I using KBr pellets. High resolution transmission electron microscope image was obtained by using a JEM-2100F (JEOL). Field Emission Scanning Electron Microsope image was obtained by using a JSM-6700F. Elemental analyses were performed by a Flash 1112 (Thermo Electron corporation). Uv-vis spectra were obtained with the use

of a SCINCO S-3150. Wide-angle X-ray diffraction (WXRD) was recorded by Bruker Xps GADDS (Cu Kα radiation, λ = 1.54 Å). Powder X-ray diffraction was recorded by Bruker D5005. X-ray photoelectron spectroscopy (XPS) data were collected on a K-Alpha X-ray photoelectron spectrometer (AXIS-HSi, KRATOS). Mass spectra were obtained by JEOL JMS-700 in the fast atom bombardment (FAB) mode.

Model Reaction. To a solution of phenylacetylene (0.100 g, 0.980 mmol) and thiophenol (0.216 g, 1.96 mmol) in DMSO-d_6 was added AIBN (0.016 g, 0.100 mmol). The solution was stirred at 100 ^{o}C and identified by ^{1}H NMR and GC-MS measurement.

Synthesis of Tetrakis(4-iodophenyl)adamantane. This compound was prepared according to the reported procedure.[104]

^{1}H NMR ($CDCl_3$, 300 MHz): δ 7.67 (d, 8H, ArH), 7.18 (d, 8H, ArH), 2.05 (s, 12H, adamantine H).

Synthesis of Tetrakis(4-ethynylphenyl)adamantane. This compound was prepared according to the reported procedure.[105] To a solution of tetrakis(4-iodophenyl)adamantane (1.00 g, 1.06 mmol) in toluene (80.0 mL),

trimethylsilylacetylene (0.416 g, 4.24 mmol), TEA (30.0 mL), CuI (25.0 mg), and dichlorobis(triphenylphosphine)palladium (50.0 mg) were added at room temperature. The solution was stirred at reflux for 10 h. After evaporation of the solvent, the product was dissolved in $CHCl_3$ (50.0 mL) and washed with water. The organic phase was dried by anhydrous magnesium sulfate. After filtration, the solvent was evaporated and the product was isolated by recrytallization from MeOH (yield: 0.850 g, 97 %). ^{1}H NMR ($CDCl_3$, 300 MHz): δ 7.44 (d, 8H, ArH), 7.38 (d, 8H, ArH), 2.05 (s, 12H, adamantine H), 0.27 (s, 36H, $SiCH_3$).

To a solution of tetrakis(4-trimethylsilylethynylphenyl)adamantane (500 mg, 0.932 mmol) in THF/MeOH (100 mL, v/v=1/1), K_2CO_3 (1.03 g, 7.45 mmol, 8eq) was added. The solution was stirred at room temperature for 10 h. After evaporation of the solvent, the product was dissolved in dichloromethane (50 mL) and washed with water. The organic phase was dried by anhydrous magnesium sulfate. After filtration, the solvent was evaporated and the product was isolated by recrytallization from MeOH (yield: 0.252 g, 77 %). ^{1}H NMR ($CDCl_3$, 300 MHz): δ 7.49 (d, 8H, ArH), 7.42 (d, 8H, ArH), 3.05 (s, 4H, CH), 2.12 (s, 12H, adamantane H).

Preparation of Microporous Networks by Thiol-yne reaction. To a solution of Tetrakis(4-ethynylphenyl)adamantane (0.126 g, 0.235 mmol) and

1,3,5-benzenetrithiol (0.109 g, 0.628 mmol) in DMF (80.0 mL), AIBN (0.154 g, 0.942 mmol) was added at room temperature. The solution was stirred at 130 ^{o}C for 2 days. The precipitated polymer was isolated by filtration and washed with THF, dichloromethane, MeOH, and water. The polymer was further purified by soxhlet-extraction with MeOH for 12 h and dried in vacuum. Yield: 0.165 g (70.2 %). Anal. Calcd for $C_{54}H_{44}S_6$: C, 73.26; H, 5.01; S, 21.73. Found: C, 64.24; H, 4.27; S, 23.79.

Preparation of Au NPs loaded Microporous Polymer. To a dispersant of microporous polymer (30.0 mg) in ethanol (5.00 mL), $HAuCl_4$ aqueous solution (1 mL, 8 mg/mL) was added. The solution was stirred at 600 rpm for 1 hour. $NaBH_4$ aqueous solution (1 mL, 25 mM) was slowly added into the solution. The color of solution changed from yellow into dark brown. After 30 min, microporous polymer was filtered and washed with ethanol and water. Au NPs loaded microporous polymer was dried in vacuum.

Catalytic Ability Study. 4-Nitrophenol was chosen as substrates for the catalytic hydrogenations in the presence of $NaBH_4$ as a hydrogen source. To a freshly prepared aqueous $NaBH_4$ solution (1 mL, 0.1 mM), 4-nitrophenol solution in EtOH (5 mL, 0.05 mM) was added at room temperature. Au NPs

loaded microporous polymer (10.0 mg) was added into the solution under gentle stirring. Uv-vis absorption spectra were recorded with regular intervals to monitor the catalytic reductions of 4-nitrophenol for 12 h.

II-3. Results and Discussion

The microporous polymer was prepared by a thiol-yne addition reaction of tetrakis-(4-ethynylphenyl)adamantine. Scheme II-1 shows the synthetic process of tetrakis(4-ethynylphenyl)adamantane. Tetraphenyladamantane was synthesized by the Fridel-Crafts reaction of 1-bromoadamantane with benzene in the presence of $AlCl_3$. The iodization reaction of tetraphenyladamantane was performed according to the previous paper.[104] Tetrakis(4-ethynylphenyl)adamantane was prepared by Sonogashira-Hagihara cross-coupling reaction of tetrakis(4-iodophenyl)adamantane with trimethylsilylacetylene followed by the deprotection reaction with K_2CO_3 in THF/MeOH.

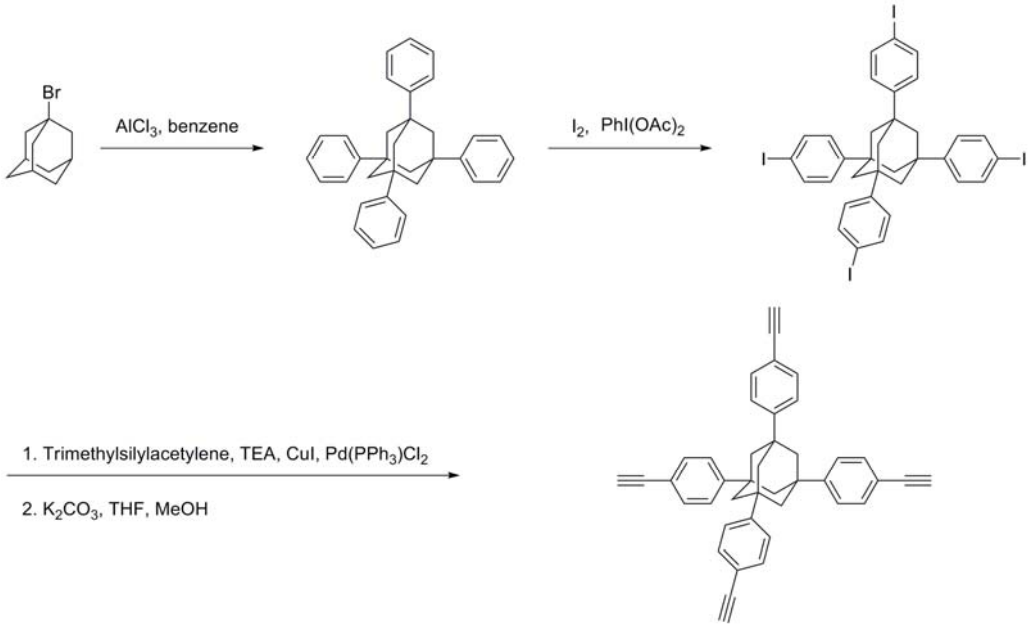

Scheme II-1. Synthesis of tetrakis(4-ethynylphenyl)adamantane.

Tetrakis(4-ethynylphenyl)adamantine was reacted with a two-fold excess of 1,3,5-benzenetrithiol in the presence of AIBN in DMF. The addition of a thiyl radical formed with AIBN to an ethynyl group yielded a vinyl linker. The disulfide groups were produced by the reaction between thiol groups. The structure of the microporous polymer was investigated by ^{13}C NMR and FT-IR spectroscopy. In the soldi state ^{13}C NMR spectrum [Figure II-1], aromatic carbon peaks were observed at 124, 133, 137 and 148 ppm. The peak of acetylene carbons at 90 ppm did not appear, indicating that all acetylene groups reacted with thiol groups. The peaks of vinyl carbons overlapped with those of

aromatic carbons. The adamantane carbon peaks were observed at 44 and 38 ppm. The FT-IR spectroscopy also confirmed the consumption of acetylene groups [Figure II-2]. The peak of carbon stretching vibration of an acetylene group at 2100 cm^{-1} did not show up. A weak stretching vibration band of an S-H group appeared at 2550 cm^{1}, indicating that some unreacted thiol groups remained.

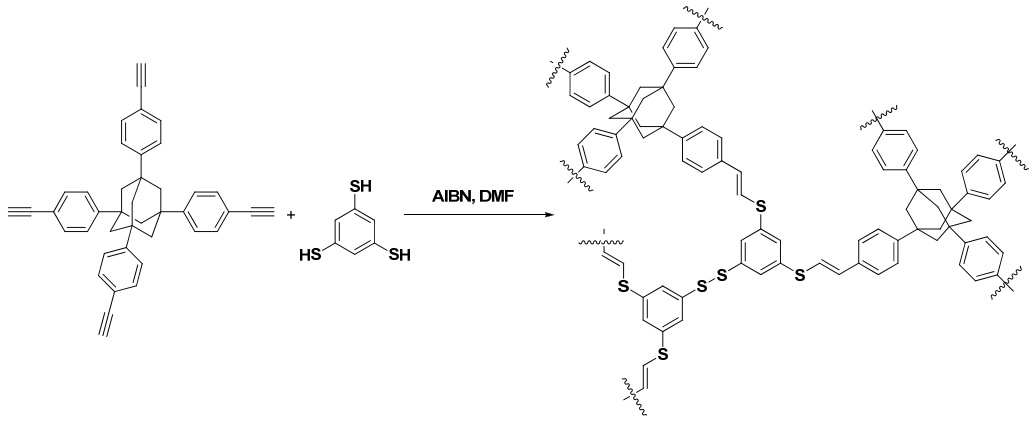

Scheme II-2. Preparation of the microporous polymer.

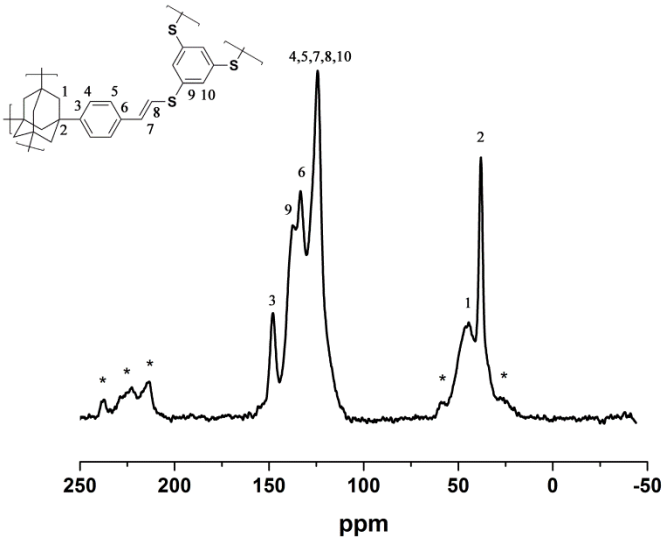

Figure II-1. Solid state ^{13}C NMR spectrum of the microporous polymer.

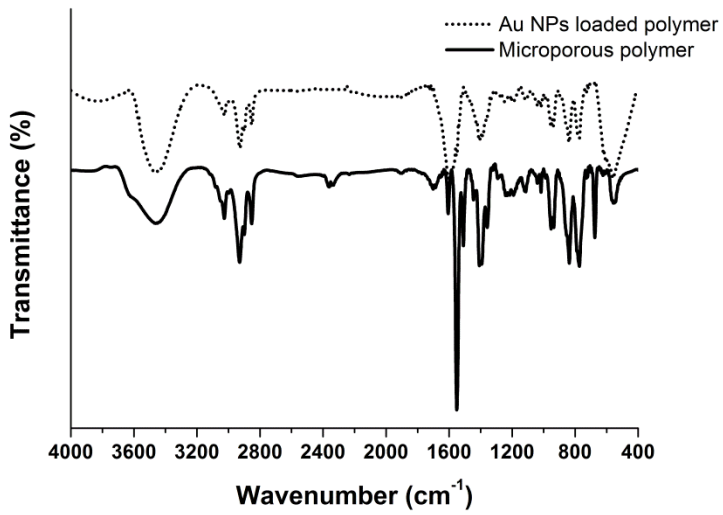

Figure II-2. FT-IR spectra of the microporous polymer and the Au loaded microporous polymer.

The model reaction for the polymerization was performed with phenylacetylene and two-fold excess of thiophenol in DMSO-d_6 as shown in Scheme II-3 and analyzed by ^{1}H NMR spectroscopy [Figure II-3]. As soon as the two chemicals were mixed [Figure II-3(a)], the thiol and acetylene peaks appeared at 5.36 and 4.18 ppm and aromatic proton peaks at 7 - 7.6 ppm. It was noteworthy that a small peak was shown at 6.68 ppm for vinylic protons, supporting the high reactivity of an activated aromatic acetylene to a thiol group in the hydrothiolation reaction.[106] After stirring at 100 ^{o}C for 3 h in the presence of AIBN [Figure II-3(b)], the vinylene peak intensity significantly increased, while the acetylene peak totally disappeared as participated in the reaction. Vinylene doublets of trans configuration appeared at 7.21 and 6.79 ppm (J = 15.6 Hz) and those of cis configuration appeared at 6.69 and 6.67 ppm (J = 10.8 Hz). A mole ratio of the trans isomer to the cis isomer was estimated to be 17 : 3.[107-109] The integration ratio of one vinylene proton to aromatic protons was calculated to be 1 : 15, indicating one acetylene was ~~almost~~ reacted with one thiol through the thiol-yne reaction. The excess thiol groups were consumed to form disulfide bonds instead of undergoing the thiol-ene reaction with vinyl sulfide groups. After the reaction for 24 h, the thiol peak completely disappeared [Figure II-3(c)].

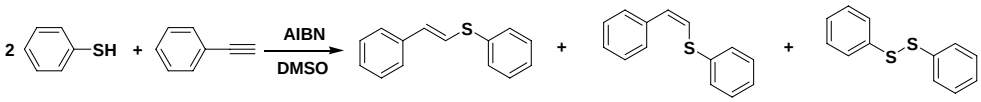

Scheme II-3. Schematic description for the model reaction with thiophenol and phenylacetylene.

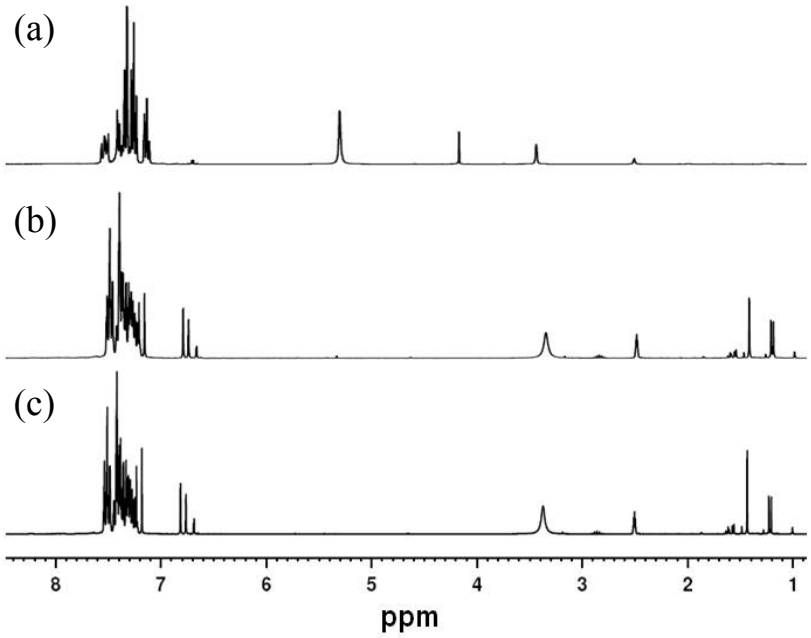

Figure II-3. ^{1}H NMR spectra of a solution of thiophenol and phenylacetylene in DMSO-d_6 measured (a) before heating without AIBN, (b) after heating with AIBN for 3 h and (c) 24 h

Scheme II-4 shows the process of preparing Au NPs in the microporous polymer. Au NPs were formed in the microporous polymer by in-situ reduction of $HAuCl_4$ precursor with $NaBH_4$ in an aqueous solution. After the reaction, the polymer was washed with water and ethanol. In the FT-IR spectrum of Au NPs loaded microporous polymer [Figure II-2], the stretching vibration band of an S-H group disappeared, indicating that the Au NPs were immobilized in the microporous polymer through interaction with sulfur atoms of the thiol groups.[110,111]

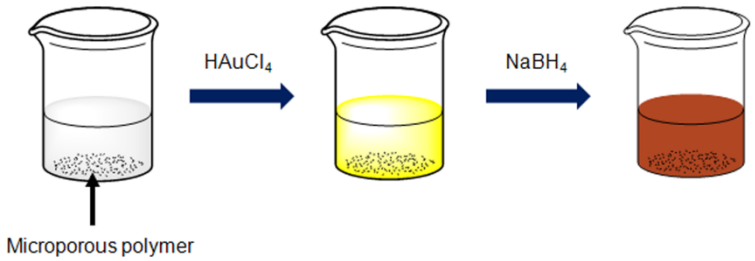

Scheme II-4. Preparation of the Au NPs loaded microporous polymer.

Figure II-4 shows the SEM image and wide-angle X-ray diffraction pattern of the microporous polymer. The microporous polymer had a spherical shape with 20 – 30 nm diameter and an amorphous structure.

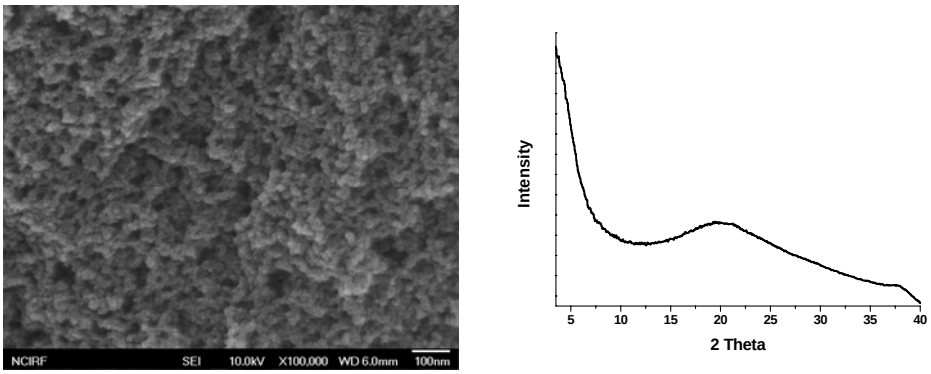

Figure II-4. SEM image and WXRD pattern of the microporous polymer.

The porosity of microporous polymer was investigated by nitrogen adsorption-desorption isotherms [Figure II-5]. The microporous polymer had a type II isotherm according to IUPAC classification. Hysteresis was observed in high pressure ranging from 0.75 to 1.0. The BET surface area was calculated in the relative pressure (P/P_0) ranging from 0.05 to 0.15. The total pore volume was obtained at the relative pressure of 0.995. The BET surface area and total pore volume of the microporous polymer were 576 m^2/g and 1.76 cm^3/g, respectively. After incorporating Au NPs, the BET surface area decreased from 576 m^2/g to 104 m^2/g because some pores were occupied by Au NPs and a weight of polymer increased. In NLDFT pore size distribution [Figure II-5(b)], no significant change was observed after Au NPs were loaded.

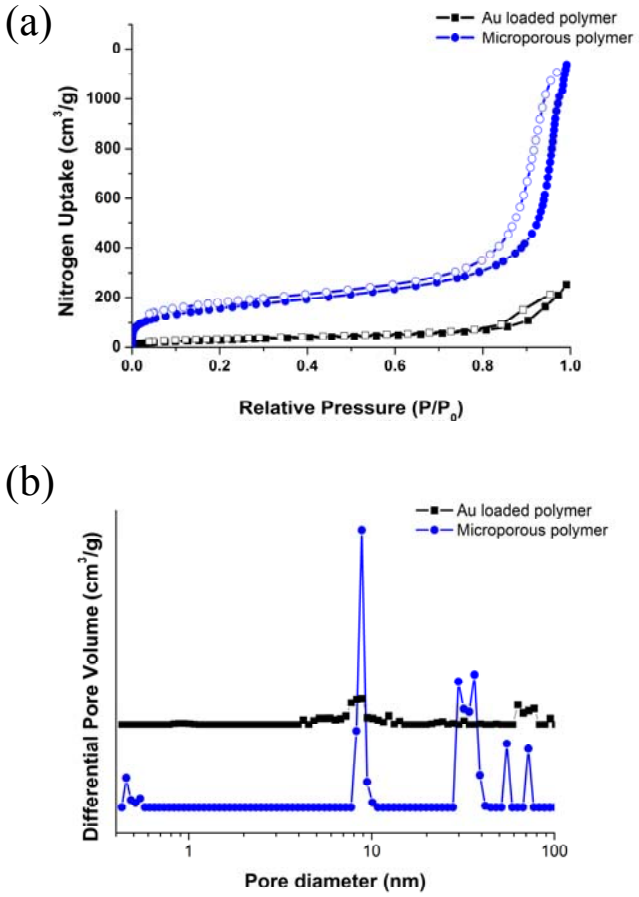

Figure II-5. (a) Nitrogen adsorption-desorption isotherms at 77 K and (b) NLDFT pore size distribution of the Au NPs loaded microporous polymer and the microporous polymer.

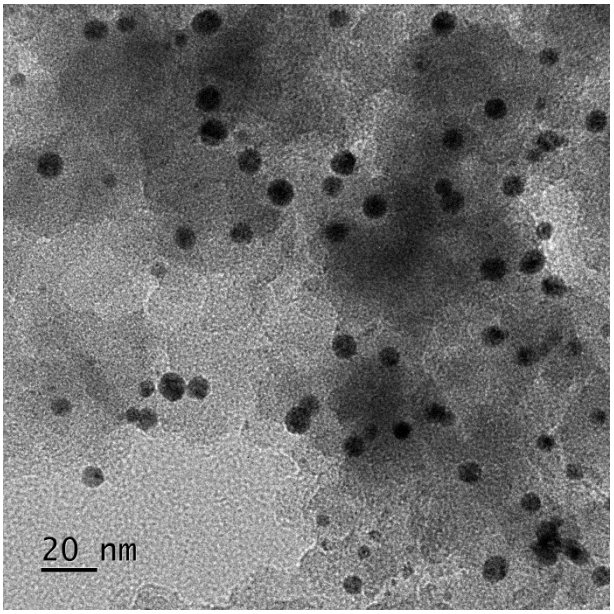

Figure II-6. HR-TEM image of Au NPs loaded microporous polymer.

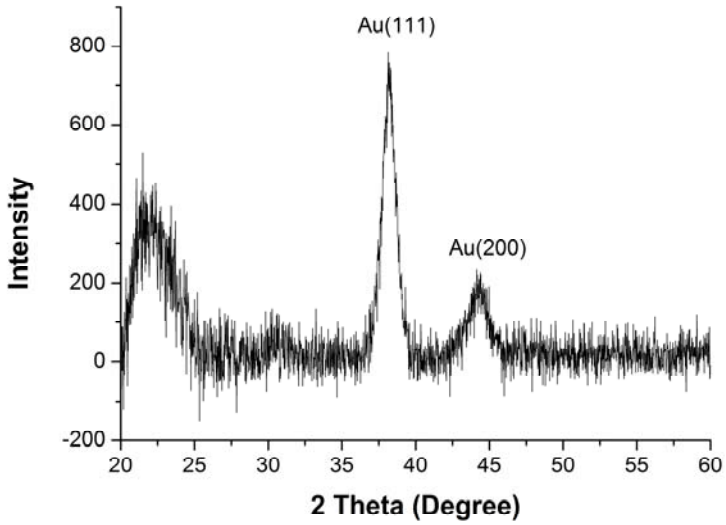

Figure II-7. Powder XRD pattern of Au NPs loaded microporous polymer.

The formation of Au NPs was confirmed by high resolution TEM. The Au NPs were well dispersed in the microporous polymer, probably bound to sulfide or thiol end groups [Figure II-6]. The average diameter of Au NPs was 7.02 nm.

The X-ray diffraction pattern of the Au NPs loaded microporous polymer showed two strong peaks at $2\theta = 38.2°$ and 44.5°, corresponding to the (111) and (200) plane, respectively, of fcc Au crystalline [Figure II-7].[94,112] The size of the Au NPs was estimated from the peak width of the (111) Bragg reflection using the Debye–Scherrer formula. The calculated average diameter of Au NPs was 7.28 nm which was consistent with the result from TEM image.

The elemental states of the Au NPs loaded microporous polymer were investigated by X-ray photoelectron spectroscopy (XPS). In the X-ray photoelectron spectrum [Figure II-8], the peaks of C 1s, S 2s, and S 2p existed at 284, 227, and 162 eV, respectively. The peaks of Au 4d binding energy were shown at 334 and 351 eV. In high-resolution XPS spectrum [Figure II-8 inset], the peaks at 84.4 and 88.2 eV corresponding to Au $4f_{7/2}$ and Au $4f_{5/2}$ binding energies, respectively, were observed.[113] The binding energies of Au 4f were slightly higher than those of bulk Au 4f ($4f_{7/2}$ = 84.0 eV and $4f_{5/2}$ =87.6 eV). No Au^{3+} binding energy peaks could be observed at about 86 and 90eV, suggesting that the unreacted $HAuCl_4$ precursor was removed successfully. The S 2p

binding energy at 162 eV was corresponding to S chemisorbed on the Au surface through a thiolate bond.[114,115]

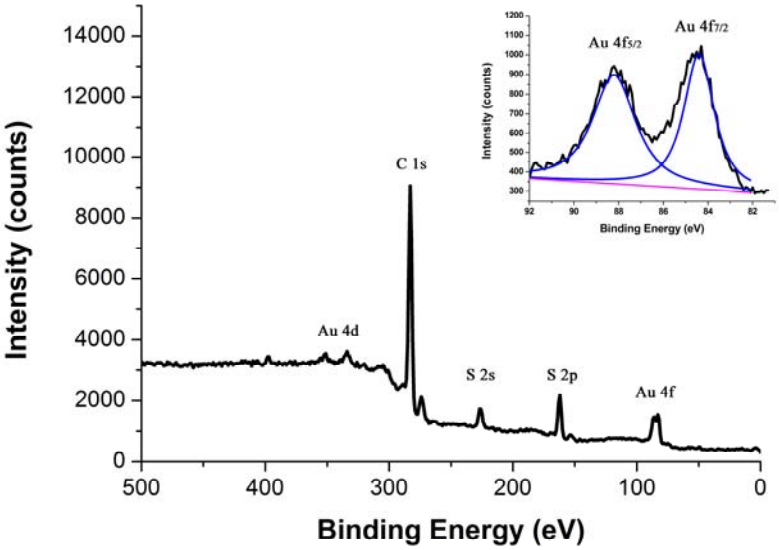

Figure II-8. X-ray photoelectron spectrum of the Au NPs loaded microporous polymer and high-resolution X-ray Photoelectron spectrum (inset).

The catalytic activity of Au NPs dispersed in the microporous polymer was evaluated using the reduction of 4-nitrophenol (4-NP) with $NaBH_4$ in an aqueous solution as a model reaction.[102-106] The reduction reaction was followed by UV-vis absorption spectroscopy [Figure II-9]. 4-NP showed a strong absorption peak at 317 nm. When $NaBH_4$ was added to the 4-NP solution, the absorption peak shifted to 400 nm, indicating the formation of 4-

nitrophenolate ions. The reaction proceeded only after the addition of the Au NPs loaded microporous polymer. The peak intensity at 400 nm from 4-nitrophenolate ions decreased with the reaction time, while a new peak at 315 nm from 4-aminophenol became stronger. After 6 h, the peak at 400 nm disappeared completely, suggesting the completion of the reaction.

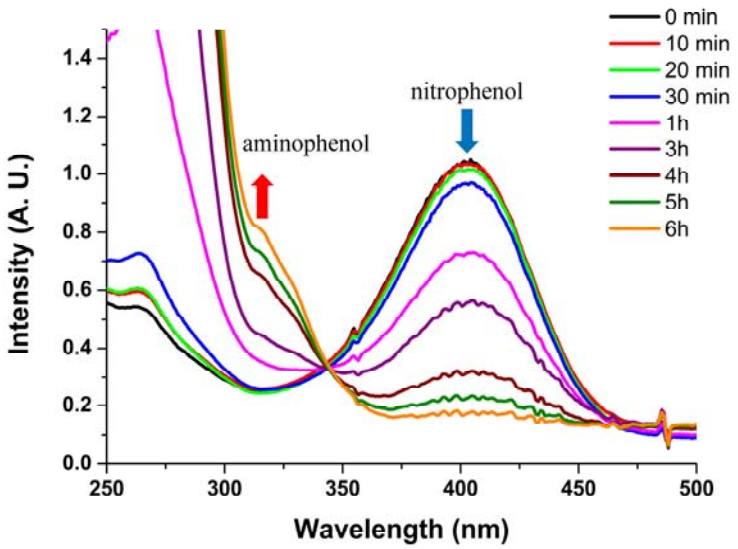

Figure II-9. Uv-vis spectra measured during the catalytic reduction of 4-nitrophenol into 4-aminophenol in the presence of the Au NPs loaded microporous polymer.

II-4 Conclusion

A microporous polymer was prepared by thiol-yne addition reaction without any metal catalyst. The microporous polymer had a BET surface area of 576 m^2/g. The unreacted thiol groups and disulfide groups were used as binding sites of Au NPs. Au NPs were produced by the reduction reaction of $HAuCl_4$ and immobilized through interactions with the sulfur groups in the polymer network. The BET surface area of the microporous polymer decreased to 104 m^2/g after incorporation of the Au NPs. The Au NPs in the polymer showed a fcc crystalline structure and their average diameter were determined to be about 7 nm by HR-TEM and XRD. The Au NPs loaded microporous polymer showed the strong catalytic activity in the reduction reaction of 4-nitrophenol with $NaBH_4$.

Chapter III. Preparation of Molecularly Imprinted Microporous Polymers by Yamamoto Cross-Coupling Reaction

III-1. Introduction

Molecular imprinting provides synthetic materials having selective molecular recognition sites efficiently and economically, mimicking the biological receptors. The preparation of a molecularly imprinted polymer involves three stpes: (1) assembly of a functional monomer and a template molecule, (2) cross-linking of the functional monomer-template assemblies, and (3) removal of the template molecules from the polymer matrix. The empty cavities become the binding sites for the template molecules.

The imprinting method can be classified into a covalent and a non-covalent method according to the kind of a bond used for the assembly of a functional monomer and a template.[116] In the covalent imprinting method pioneered by Wulff and coworker, a template and a functional monomer are linked by a covalent bond to form a template-functional monomer complex.[117] The monomer-template complex is polymerized in the presence of a cross-linker and then the template molecules are removed from the polymer in harsh conditions. The non-covalent imprinting method uses non-covalent interactions such as hydrogen bonding, electrostatic interaction, π–π interaction, and hydrophobic interaction for the formation of a monomer-template complex.[118] After polymerization, the template molecules are easily removed under mild

conditions.

Bisphenol-A is known as an endocrine disruptor that can cause adverse effects on humans and wild life through interactions with the endocrine system. Due to the increased awareness of the risks involved with endocrine disrupting compounds, the ability to detect bisphenol-A is of great importance.[119]

A bisphenol-A imprinted microporous polymer was preprared by Yamamoto cross-coupling reaction. Bisphenol-A was connected to two 4-bromophenyl groups through thermally reversible urethane bonds. The urethane groups could dissociate reversibly at elevated temperatures. Yamamoto cross-coupling reaction of tetrakis(4-bromophenyl)methane and the bisphenol-A complex provided the microporous polymer containing bisphenol-A, which was extracted easily by simple heating in 1,4-dioxane/H_2O. The rebinding ability of the imprinted polymer was investigated.

III-2. Experimental

Materials. Bisphenol-A, 4-bromophenyl isocyanate, 1,5-cyclooctidiene, 2,2'-bipyridyl, bis(1,5-cyclooctadiene) nickel(0), bromine, 4,4'-biphenol, and diethylstilbestrol were purchased from Aldrich and used as received. Tetraphenylmethane was purchased from Alfa Aesar and used as received. Tetrahydrofuran (THF) was used after purification by standard methods. Other reagent-grade solvents were used as received.

Measurements. N_2 uptake amounts were measured by using a Belsorp-Max (BEL Japan, Inc.) apparatus. Ultra-high purity grade $N_2$was used for all adsorption measurements. ^{1}H nuclear magnetic resonance (NMR) spectra were measured by a Bruker Avance DPX-300 (300 MHz for ^{1}H NMR) spectrometer. All chemical shifts were listed in ppm downfield from tetramethylsilane (^{1}H NMR). ^{13}C Solid state NMR measurements were carried out on a Bruker 400 Solid/Micro-Imaging High Resolution NMR with resonance frequencies of 100 MHz. Fourier transform infrared (FT-IR) measurements were recorded on a PERKIN ELMER Spectrum GX I using KBr pellets. Transmission electron microscopy (TEM) images were obtained by a JEM1010 (JEOL). Field Emission Scanning Electron Microsope image was obtained by using a JSM-

6700F.Wide-angle X-ray diffraction (WXRD) was recorded by Bruker Xps GADDS (Cu Kα radiation, λ = 1.54 Å). Differential scanning calorimetry (DSC) measurement was performed by a TA modulated DSC Q10 with a scanning rate of 3 ^{o}C/min under nitrogen. HPLC analysis was carried out using a M930 solvent delivery system, a M720 UV-vis detector (YOUNGLIN Instrument Co., Ltd., Korea), a MetaSil 5 μm ODS column from Metachem (Torrance, Canada) with methanol as an eluent at a rate of 1.0 mL/min at 40 ^{o}C.

Synthesis of BisA-Br. To a solution of bisphenol-A (0.5 g, 2.19 mmol) and 4-bromophenyl isocyanate (0.867 g, 4.38 mmol) in dry THF (50 ml), dibutyltin diarurate (0.1 mL) was added. After reflux for 12 h, the solvent was evaporated. The crude product was purified by column chromatography with THF/HX (1/4=v/v) as an eluent. The product was dried in vacuum. Yield: 64 %. ^{1}H NMR (300 MHz, $CDCl_3$): δ 8.53 (s, 1H, NH),8.40 (d, 2H, ArH), 8.04 (d, 2H, ArH), 7.56 (d, 2H, ArH), 7.50 (d, 2H, ArH), 1.53 (s, 6H, CH_3). FT-IR (KBr pellet): 3054, 2923, 2853, 1718, 1522, 1448, 1257, 1097, 882, 728, 534.

Synthesis of Imprinted Microporous Polymer. To a solution of tetrakis(4-bromophenyl)methane (0.550 g, 0.864 mmol) and BisA-Br (0.12 g, 0.0962 mmol) in dry THF, 1,5-cyclooctadiene (0.494 mL, 4.02 mmol), 2,2'-bipyridyl

(0.626 g, 4.02 mmol), and bis(1,5-cyclooctadiene) nickel(0) (1.10 g, 4.02 mmol) were added. The solution was stirred at room temperature for 12 h. The precipitated polymers were isolated by filtration and washed with methanol, acetone and DMF. Resulting polymer was dried in vacuum at room temperature for 2 days. Yield: 0.28 g.

Extraction of Template from Imprinted Microporous Polymer. The microporous polymer (0.25 g) dispersant in a mixture of 1,4-dioxane/H_2O (19/1 = v/v) was refluxed for 24 h. The precipitated polymers were isolated by filtration and washed with methanol, acetone and DMF. The polymer was further purified by soxhlet-extraction with methanol for 12 h and dried in vacuum at 150 ^{o}C for 24 h. Yield: 0.175 g. FT-IR (KBr pellet): 3071, 3028, 1603, 1490, 1251, 1183, 1076, 1005, 810, 763.

Synthesis of Non-imprinted Microporous Polymer. To a solution of tetrakis(4-bromophenyl)methane (0.318 g, 0.500 mmol) in dry THF, 1,5-cyclooctadiene (0.247 mL, 2.01 mmol), 2,2'-bipyridyl (0.313 g, 2.01 mmol), and bis(1,5-cyclooctadiene) nickel(0) (0.552 g, 2.01 mmol) were added. The solution was stirred at room temperature for 12 h. The precipitated polymers were isolated by filtration and washed with methanol, acetone and DMF. The

polymer was further purified by soxhlet-extraction with dichlomethane for 24 h and dried in vacuum at 150 ^{o}C. Yield: 0.154 g. ^{13}C CP/MAS NMR (100 MHz): δ 146, 140, 131, 125, 64. FT-IR (KBr pellet): 3091, 3034, 1605, 1493, 1385, 1262, 1193, 1121, 1005, 917, 811, 749, 704.

Rebinding Test. In specific binding test, the imprinted microporous polymer or the control polymer was added to the 0.5 mM solutions of bisphenol-A, diethylstilbestrol, 4,4'-biphenol in THF (10 mL). After incubating for 3 h at room temperature, the microporous polymers were isolated by filtration. The filtrate was analyzed by HPLC.

In kinetic test, the imprinted microporous polymer or the control polymer was added to the 0.5 mM solutions of bisphenol-A, diethylstilbestrol, 4,4'-biphenol in THF (10 mL). Then, 0.4 mL of the mixture was taken at regular time and filtered. The filtrate was analyzed by HPLC.

III-3. Results and Discussion

The template-monomer complex, BisA-Br was synthesized according to Scheme III-1. 4-Bromophenyl isocyanate was reacted with bisphenol-A in the presence of dibutyltin diarurate as a catalyst in dry THF. In the complex, the template was connected to two bromophenyl functional groups through a thermally reversible urethane bond. The urethane bond formed between an isocyanate group and a phenol group was stable at room temperature, however, it was cleaved at elevated temperatures. The BisA-Br was analyzed by ^{1}H NMR and FT-IR spectroscopy. The FT-IR spectrum of BisA-Br showed a peak at 1718 cm^{-1} for C=O stretching vibration of a urethane bond.

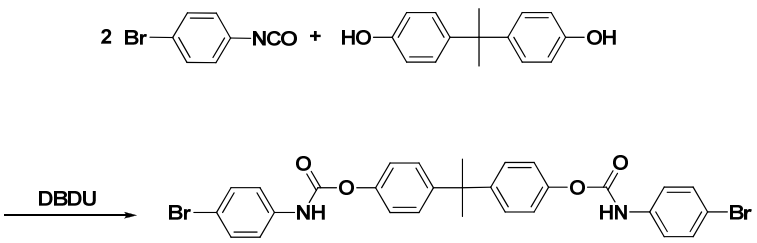

Scheme III-1. Synthesis of BisA-Br.

The microporous polymer was prepared by Yamamoto cross-coupling reaction of tetrakis(4-bromophenyl)methane and BisA-Br with a ratio of 9:1 in dry THF [Scheme III-2]. The template molecules, bisphenol-A, were removed

by reflux the polymer in a mixture of 1,4-dioxane and H_2O. In the process of the extraction, isocyanate groups would be regenerated by dissociation of the urethane bonds and immediately be reacted with water to produce amine groups.[120]

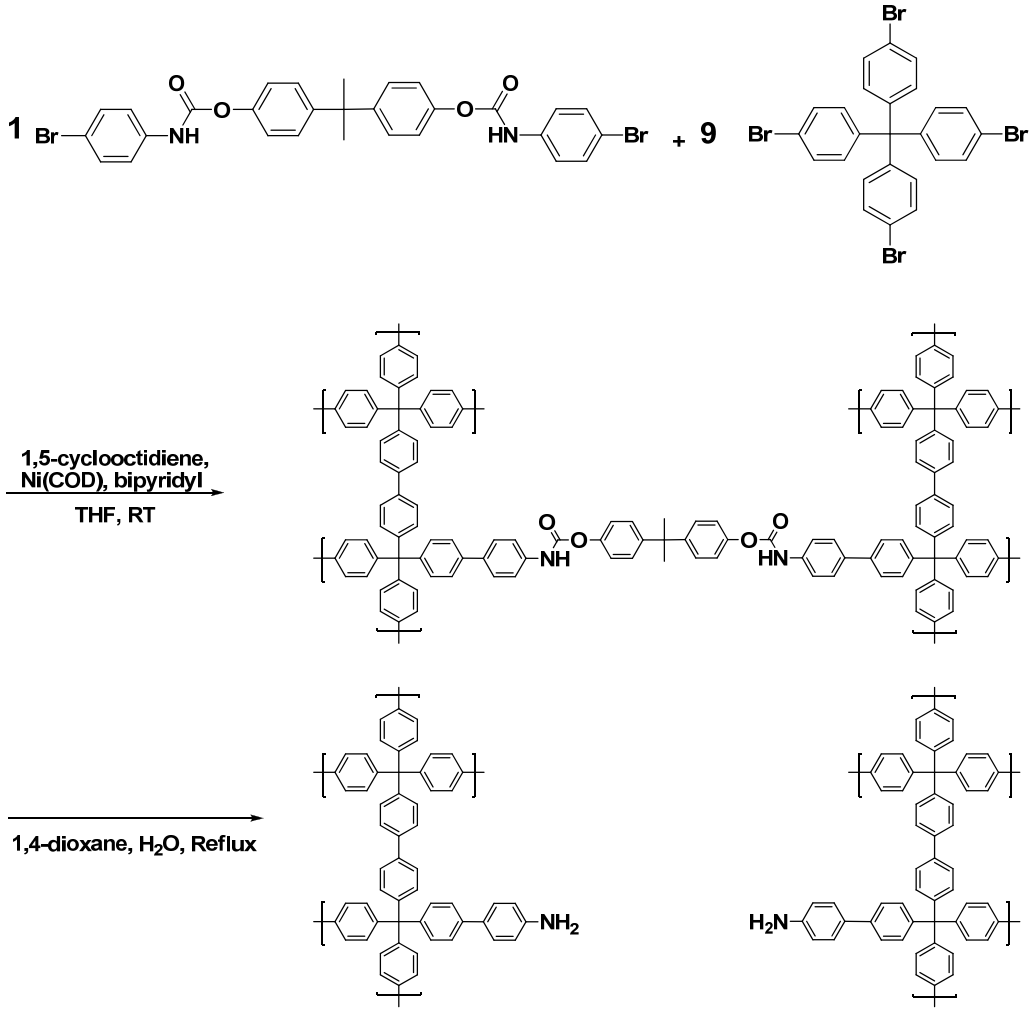

Scheme III-2. Synthesis of the imprinted microporous polymer.

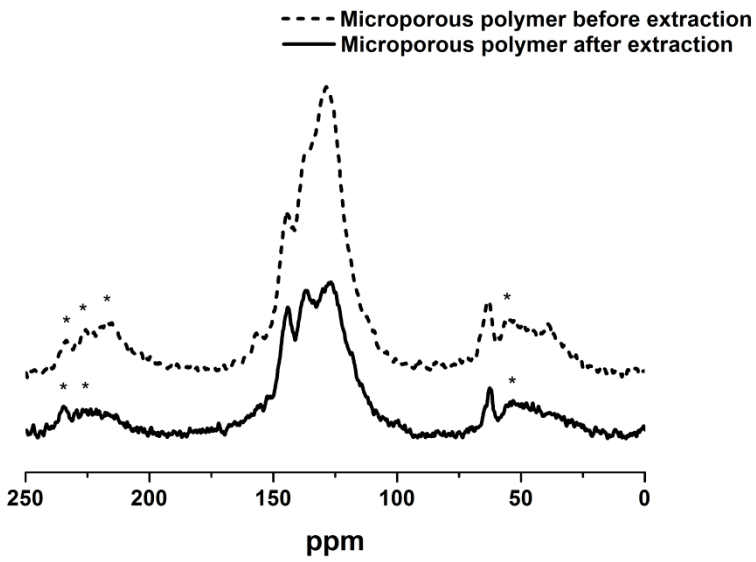

Figure III-1. ^{13}C CP/MAS NMR spectra of the imprinted microporous polymer before and after extraction. The asterisk marks a rotational side band.

The structure of the polymers was characterized by ^{13}C CP/MAS NMR spectroscopy [Figure III-1]. In the spectra of the microporous polymer obtained before and after extraction, the peaks of aromatic carbons were observed at around 127, 137 and 144 ppm. The peak for a methane carbon of the tetraphenylmethane core appeared at 62 ppm. Before extraction, the tetrahedral carbon of bisphenol-A and urethane carbon peaks appeared at 38 and 155 ppm, respectively. These peaks disappeared after extraction, which indicated that the bisphenol-A was successfully removed.

The morphology of the imprinted and non-imprinted polymers was investigated by SEM and TEM. In the SEM images [Figure III-2], the imprinted and non-imprinted polymers showed the aggregates of spherical nanoparticles, which had a diameter of 100 – 200 nm. The TEM images [Scheme III-3] of the microporous polymers also showed the aggregates of small nanoparticles.

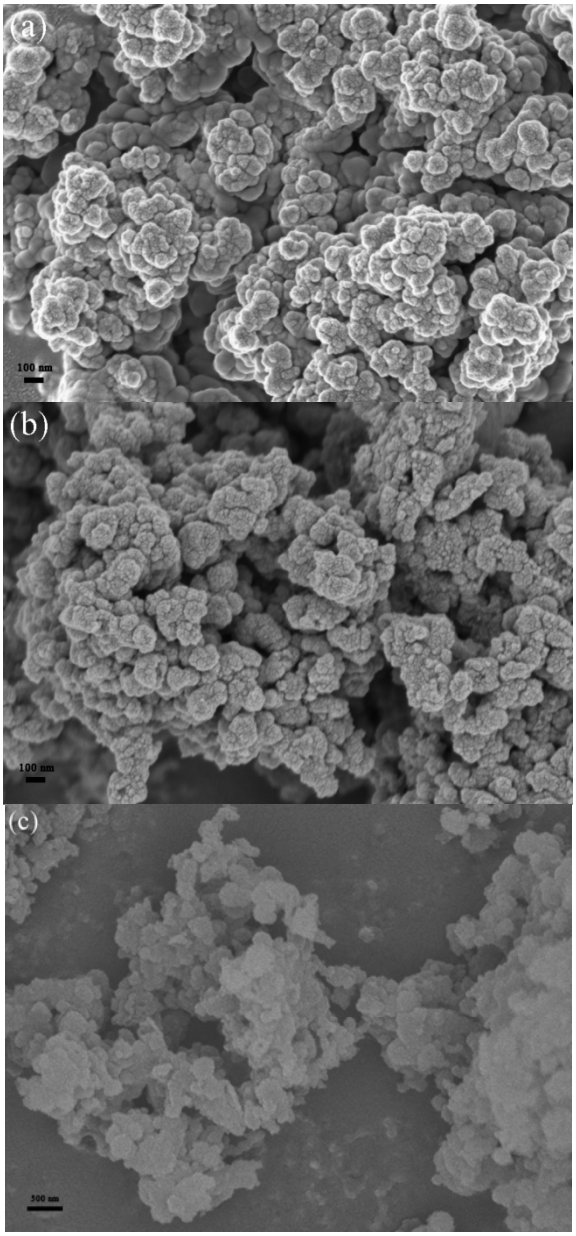

Figure III-2. SEM images of (a) the microporous polymer before extraction and (b) after extraction, and (c) the non-imprinted microporous polymer.

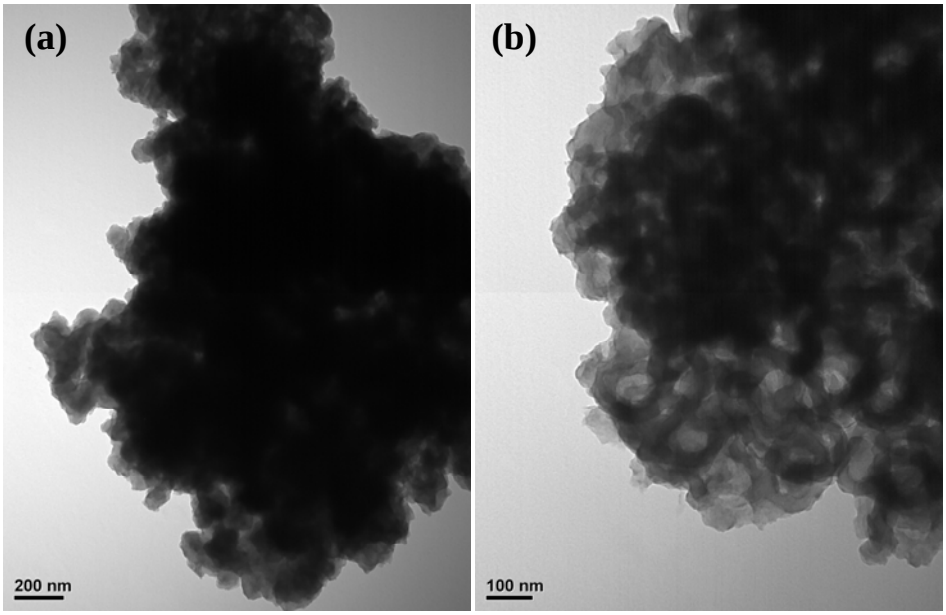

Figure III-3. TEM images of (a) the microporous polymer before extraction and (b) after extraction.

In order to probe the long-range structure of the polymer, wide angle X-ray diffraction (WXRD) studies were performed [Figure III-4]. The WXRD pattern of the polymer before and after extraction showed the peak at 2θ = 6.4°and 12.86°, corresponding to the (111) and (222) planes, respectively, of the diamond structure.[47]

The DSC analysis of the polymer was carried out to check a dissociation of the urethane functional groups [Figure III-5]. The broad endothermic peak was observed at around 130 ^{o}C before extraction. This endothermic peak indicated

that the urethane bonds in the polymer were cleaved into the isocyanate groups and phenol groups.

The porosity properties of the microporous polymers were analyzed by nitrogen adsorption-desorption analysis at 77 K [Figure III-6(a)]. The BET surface area of the microporous polymer was 25.3 m^2/g before extraction and increased to 562 m^2/g after extraction. This result was attributed to that the removal of template molecules produced more micropores and decreased the total weight of the polymer.

The pore size distributions of the microporous polymer were investigated by the NLDFT method from the nitrogen adsorption-desorption isotherms [Figure III-6(b)]. After extraction of the template molecules, more micropores with a diameter of less than 2 nm were observed. The dominant pore size was 0.733 nm.

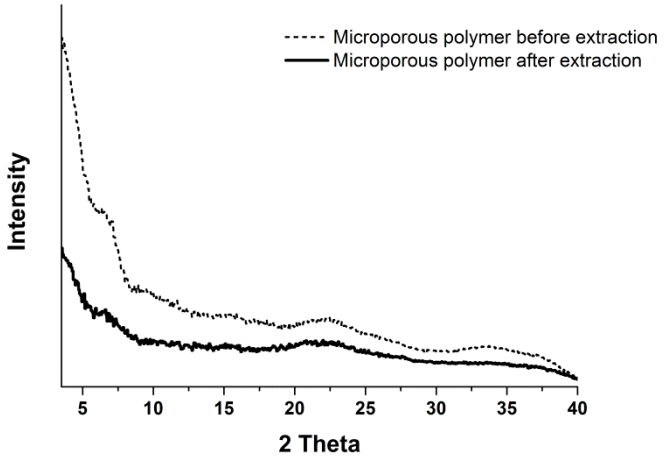

Figure III-4. Wide angle X-ray diffraction patterns of the the microporous polymer before and after extraction.

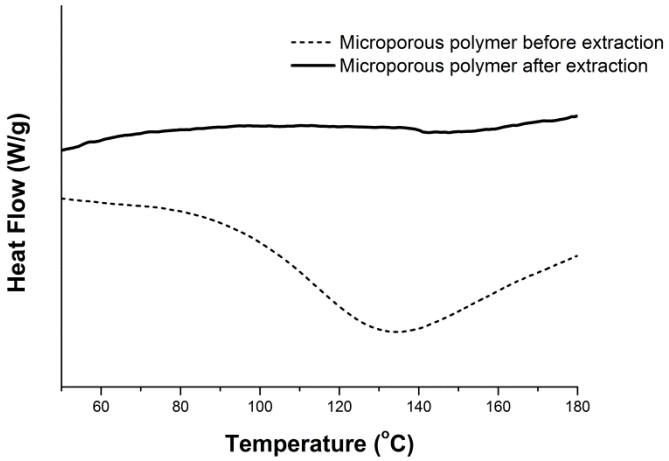

Figure III-5. DSC thermograms of the microporous polymer before and after extraction.

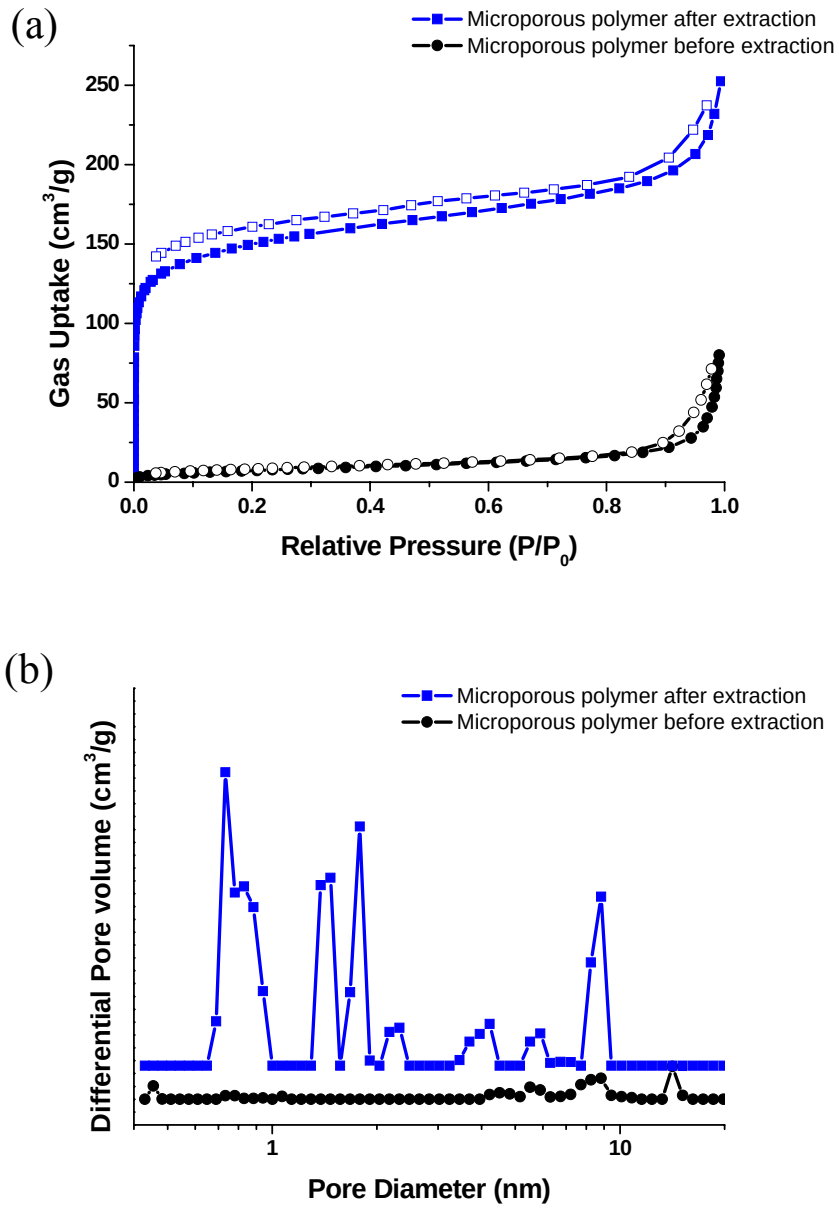

Figure III-6. (a) N_2 adsorption-desorption isotherms at 77 K and (b) NLDFT pore size distributions of the microporous polymer before and after extraction.

The rebinding properties of the imprinted microporous polymer and the control polymer were studied. The imprinted polymer or the control polymer (10 mg) was added to a solution of bisphenol-A in THF (0.5 mM, 10 mL) at room temperature. After 3 h, the concentration of bisphenol-A in the solution was measured by HPLC.

The non-imprinted microporous polymer was prepared by Yamamoto cross-coupling reaction of only tetrakis(4-bromophenyl)methane in dry THF at room temperature. The non-imprinted microporous polymer had a very high BET surface area of 5,260 m^2/g. This was used as control polymer for rebinding experiment.

Figure III-7 shows the amount of the template bound to the imprinted microporous polymer and to the control polymer according to the sample concentration. The imprinted microporous polymer exhibited much higher recognition ability than the control polymer. The superior rebinding ability of the imprinted polymer, compared with the control polymer, proved that the target molecules were not simply adsorbed at the surface, but were trapped in the cavities through hydrogen bonding. The specific recognition ability of the imprinted microporous polymer for its analogues (diethylstilbestrol and 4,4'-biphenol) was investigated. The imprinted microporous polymer had the highest recognition ability for bisphenol-A.

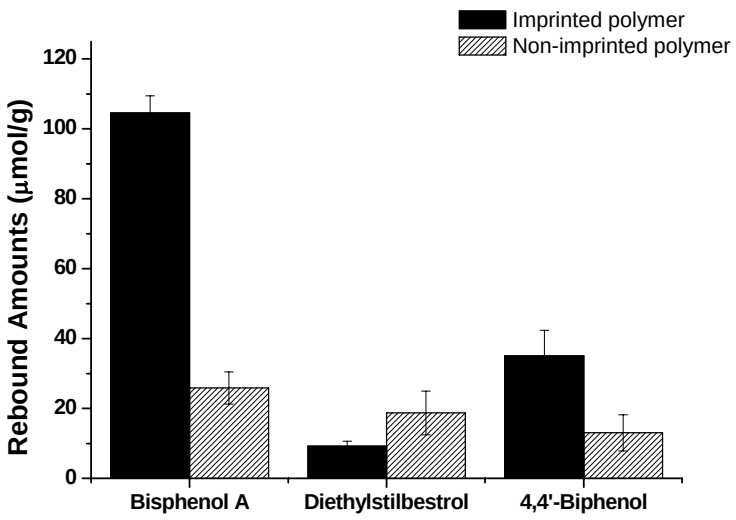

Figure III-7. Binding selectivity of the imprinted microporous polymer and the control polymer.

The kinetic uptake of bisphenol-A by the imprinted polymer was measured to evaluate the binding site accessibility [Figure III-8]. Above 90 % of an equilibrium amount was recognized within 5 min after the addition of the polymer to the bisphenol-A solution. The recognition time was much faster than that of typical molecularly imprinted materials. This result could be attributable to the fact that the binding sites were accessible through the pores in the polymer.

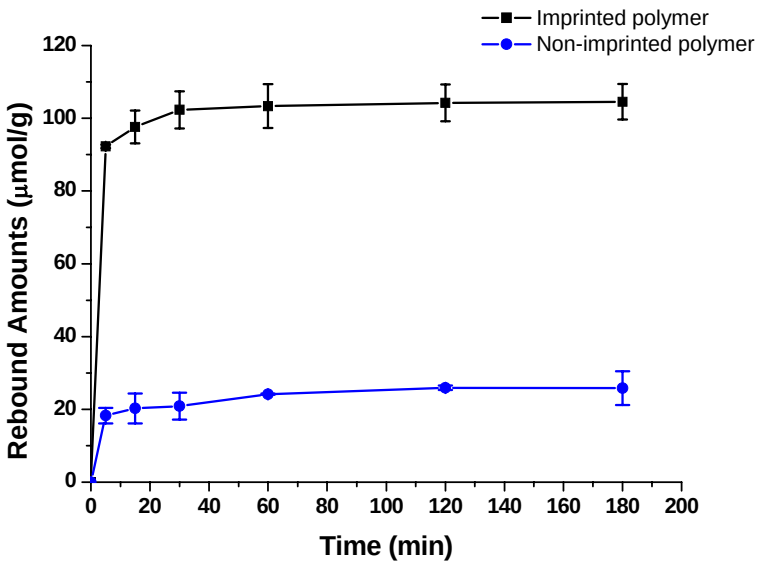

Figure III-8. Kinetic binding profiles of bisphenol-A to the imprinted microporous polymer and the control polymer.

III-4. Conclusion

A molecular imprinted microporous polymer was prepared by Yamamoto cross-coupling reaction. The thermally reversible urethane bond was used in the preparation of the template-monomer complex. The imprinted polymer showed a high and fast rebinding ability for bisphenol-A. A 90 % of an equilibrium amount was recognized within 5 min after the addition of bisphenol-A.

Chapter IV. Preparation of Microporous Polymers Consisting of Tetraphenylethene and Alkyne Units

IV-1. Introduction

Sonogashira-Hagihara cross-coupling reaction has been widely used for the synthsis of MOPs. After Cooper and his coworkers firstly reported CMP-1 by Sonogashira-Hagihara cross-coupling reaction, a variety of building blocks based on such as triphenylbenzene, triphenyltriazine, tetraphenylmethane and tetraphenyladamantane were used to form MOPs by this reaction. The microporosity of the MOPs was found to be much dependent on the structures of the building blocks.[35,36,67,68,104,121-123]

Tetraphenylethylene is well known for aggregation-induced emission and 2-dimensional structure.[124] This compound could be a good building block for MOPs because of its conjugated rigid structure. Jiang and his coworkers reported the microporous polymer (TPE-CMP) prepared by Yamamoto cross-coupling of tetrakis(4-bromophenyl)ethene.[125] The TPE-CMP network prevented the rotation of tetraphenylethene units to have the luminescent property. The same group also reported the core-shell type microporous polymers by Suzuki cross-coupling reaction of benzene-1,4-diboronic acid with 1,2,4,5-tetrabromobenzene or tetrakis(4-bromophenyl)ethene.[126]

In this study, microporous polymers consisting of tetraphenylethene and alkyne units were prepared by Sonogashira-Hagihara cross-coupling reaction of

tetrakis(4-iodophenyl)ethene with ethynylbenzene derivatives such as 1,4-diethynylbenzene, 1,3,5-triethynylbenzene, and tetrakis(4-ethynylphenyl)adamantane and their pore structures and gas uptake capacities were investigated.

IV-2. Experimental

Materials. 1,1,2,2-Tetraphenylethene, 1,4-diethynylbenzene, 1,3-diethynylbenzene, CuI, dichlorobis(triphenylphosphine)palladium(II) were purchased from Aldrich and used as received. 1,3,5-Triethynylbenzene and iodine was purchased from TCI and used as received. Other reagent-grade solvents were used as received.

Measurements. ^{1}H NMR spectra were recorded on a Bruker Avance 300 spectrometer (300 MHz). ^{13}C Solid state NMR measurements were carried out on a Bruker 400 Solid/Micro-Imaging High Resolution NMR (100 MHz).Fourier transform infrared (FT-IR) measurements were made on a PERKIN ELMER Spectrum GX I using KBr pellets. Field emission scanning electron microsope images were obtained by using a JSM-6700F. Wide-angle X-ray diffraction (WXRD) patterns were recorded by Bruker Xps GADDS (Cu Kα radiation, λ = 1.54 Å).N_2, H_2, and CO_2 uptake amounts were measured by using a Belsorp-Max (BEL Japan, Inc.) apparatus. Ultra-high purity grade N_2, H_2, and CO_2were used for all adsorption measurements.

Synthesis of Tetrakis(4-iodophenyl)ethene (TIPE). This compound was prepared according to the reported procedure.[127] ^{1}H NMR ($DMSO_{d-6}$, 300 MHz): δ 7.54 (d, 8H, ArH), 6.75 (d, 8H, ArH).

Synthesis of Tetrakis(4-ethynylphenyl)adamantane. This compound was prepared according to the reported procedure.[105] To a solution of tetrakis(4-iodophenyl)adamantane (1.00 g, 1.06 mmol) in toluene (80 mL) were added trimethylsilylacetylene (0.416 g, 4.24 mmol), TEA (30 mL), CuI (25.0 mg), and dichlorobis(triphenylphosphine)palladium (50.0 mg) at room temperature. The solution was stirred at reflux for 10 h. After evaporation of the solvent, the product was dissolved in $CHCl_3$ (50 mL) and washed with water. The organic phase was dried by anhydrous magnesium sulfate. After filtration, the solvent was evaporated and the product was isolated by recrytallization from MeOH (yield: 0.850 g, 97 %). ^{1}H NMR ($CDCl_3$, 300 MHz): δ 7.44 (d, 8H, ArH), 7.38 (d, 8H, ArH), 2.05 (s, 12H, adamantine H), 0.27 (s, 36H, $SiCH_3$).

Tetrakis(4-trimethylsilylethynylphenyl)adamantane (500 mg, 0.932 mmol) was dissolved in THF/MeOH (100 mL, v/v=1/1). After addition of K_2CO_3 (1.03 g, 7.45 mmol, 8eq), the solution was stirred at room temperature for 10 h. After evaporation of the solvent, the product was dissolved in dichloromethane (50 mL) and washed with water. The organic phase was dried by anhydrous

magnesium sulfate. After filtration, the solvent was evaporated and the product was isolated by recrytallization from MeOH (yield: 0.252 g, 77 %). ^{1}H NMR ($CDCl_3$, 300 MHz): δ 7.49 (d, 8H, ArH), 7.42 (d, 8H, ArH), 3.05 (s, 4H, CH), 2.12 (s, 12H, adamantane H).

Preparation of TPE-DB. To a solution of TIPE (400 mg, 0.478 mmol) and 1,4-diethynylbenzene (0.121 g, 0.957 mmol) in DMF (80 mL) were added TEA (30 mL), CuI (25.0 mg), and dichloro(triphenylphosphine)palladium(II) (50.0 mg) at room temperature. The solution was stirred at 80 ^{o}C for 12 h. The precipitated polymer was isolated by filtration and washed with THF, dichloromethane, MeOH, and water. The polymer was further purified by soxhlet-extraction with MeOH for 12 h and dried in vacuum. Yield: 0.325 g (117 %).

Preparation of TPE-TB. The polymer was prepared in the same manner as the preparation of TPE-DB. From TIPE (400 mg, 0.478 mmol) and 1,3,5-triethynylbenzene (96.1 mg, 0.637 mmol), 180 mg of the polymer was obtained (yield: 102.8%).

Preparation of TPE-AD. The polymer was prepared in the same manner as the preparation of TPE-DB. From TIPE (200 mg, 0.239 mmol) and tetrakis(4-ethynylphenyl)adamantane (128 mg, 0.239 mmol), 0.214 g of the polymer was obtained (yield: 104.0%).

Preparation of TPE-DB/TB(1:2). The polymer was prepared in the same manner as the preparation of TPE-DB. From TIPE (500 mg, 0.598 mmol), 1,4-diethynylbenzene (37.7 mg, 0.299 mmol), and 1,3,5-triethynylbenzene (89.8 mg, 0.598 mmol), 310 mg of the polymer was obtained (yield: 96.4 %).

Preparation of TPE-DB/TB(3:2). The polymer was prepared in the same manner as the preparation of TPE-DB. From TIPE (0.5 g, 0.598 mmol), 1,4-diethynylbenzene (0.0755 g, 0.598 mmol), and 1,3,5-triethynylbenzene (0.0599 g, 0.399 mmol), 0.378 g of the polymer was obtained (yield: 109.6 %).

IV-3. Results and Discussion

Scheme IV-1 shows the synthetic processes of microporous polymers TPE-DB, TPE-TB, and TPE-AD. TIPE was synthesized by iodization of 1,1,2,2-tetraphenylethene with I_2 and bis(triacetoxy)iodobenzene at room temperature.[127] TPE-DB, TPE-TB, and TPE-AD were prepared by Sonogashira-Hagihara cross-coupling reaction of TIPE with 1,4-diethynylbenzene (DB), 1,3,5-triethynylbenzene (TB), and tetrakis(4-ethynylphenyl)adamantane (AD), respectively. The reaction was carried out in DMF using dichlorobis(triphenylphosphine)palladium(II) and CuI as co-catalysts. The molar ratio of an ethynyl group to an iodine group was 1 : 1 in all three reactions. The polymer yields were above 100% probably because of unreacted halogens.[31,32] Polymers TPE-DB/TB(1:2) and TPE-DB/TB(3:2) having two different ethynyl units were obtained by using mixtures of 1,4-diethynylbenzene and 1,3,5-triethynylbenzene in molar ratios of 1 : 2 and 3 : 2, respectively, for the coupling reaction with TIPE [Scheme IV-2].

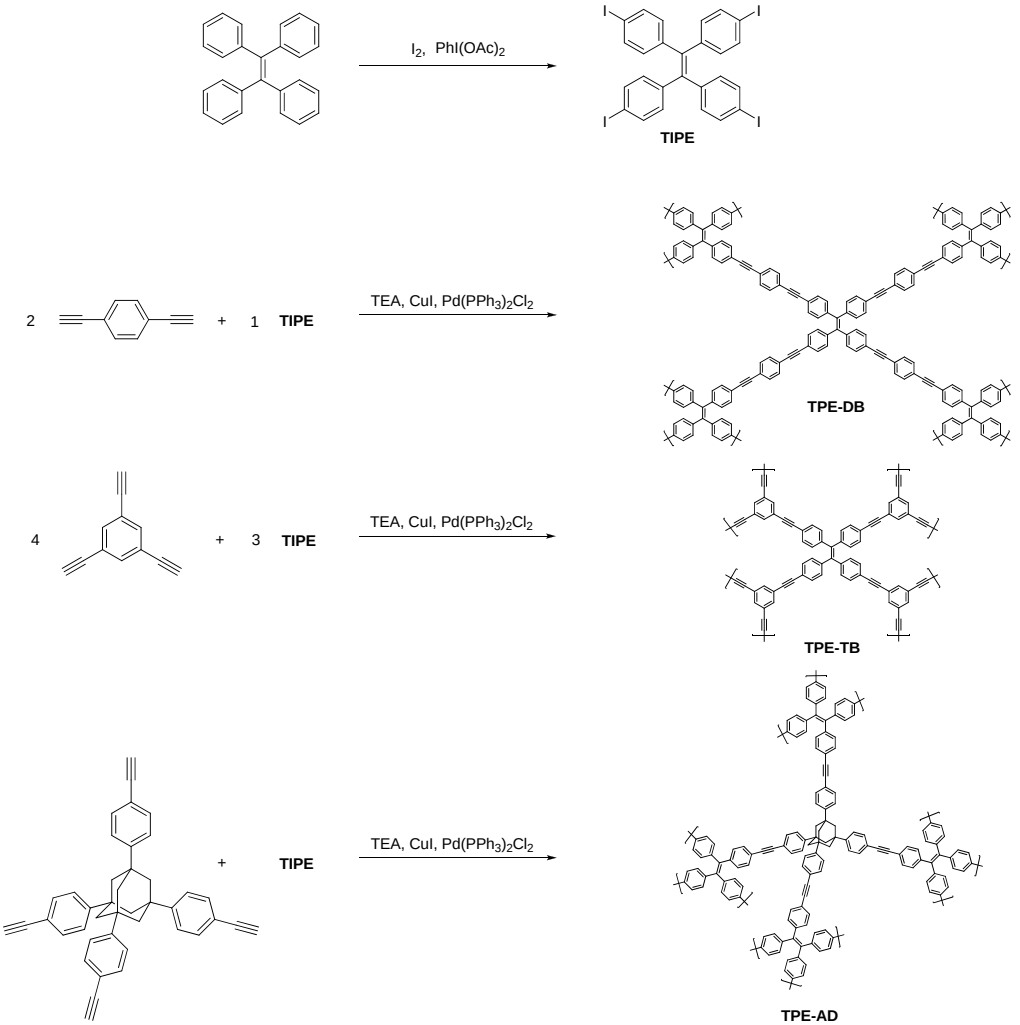

Scheme IV-1. Synthesis of microporous polymers TPE-DB, TPE-TB, and TPE-AD.

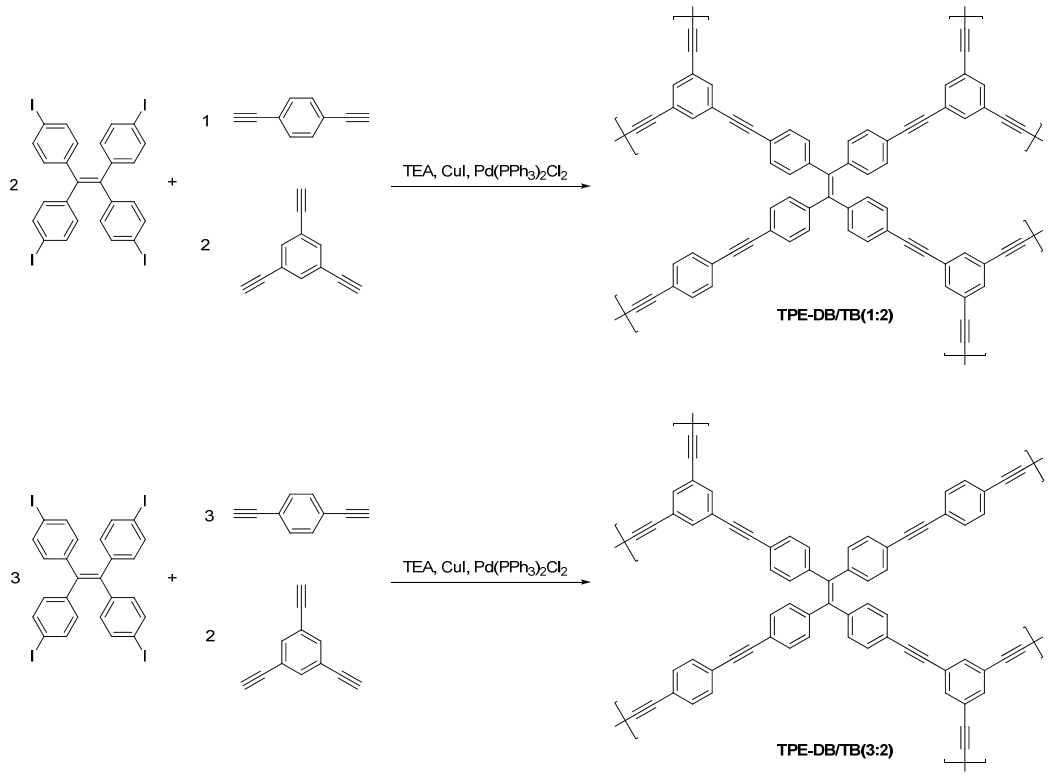

Scheme IV-2. Synthesis of microporous polymers TPE-DB/TB(1:2) and TPE-DB/TB(3:2) having two different ethynyl units.

The structures of the polymers were investigated by ^{13}C CP/MAS NMR and FT-IR spectroscopy. In solid state ^{13}C NMR spectra [Figure IV-1], the peak of acetylene carbons appeared at 90 ppm. The aromatic carbon peaks of tetraphenylethene and ethynylbenzene derivatives appeared at 120 – 140 ppm. The ethylene carbon peak of tetraphenylethene units was observed at 140 ppm. The carbon peaks of adamantane rings appeared at 44 and 37 ppm [Figure IV-

1(c)]. In the FT-IR spectra of the polymers, the peaks of stretching vibrations of carbon–carbon triple bonds and aromatic C–H stretching vibrations appeared at around 2200 cm^{-1} and 3030 – 3060 cm^{-1}, respectively.

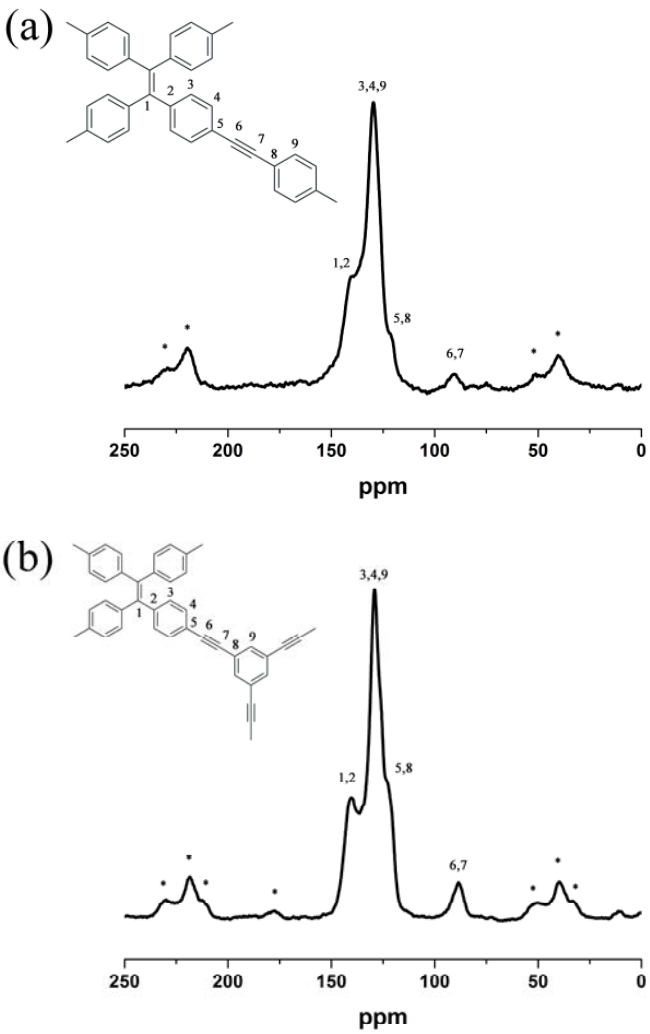

(c)

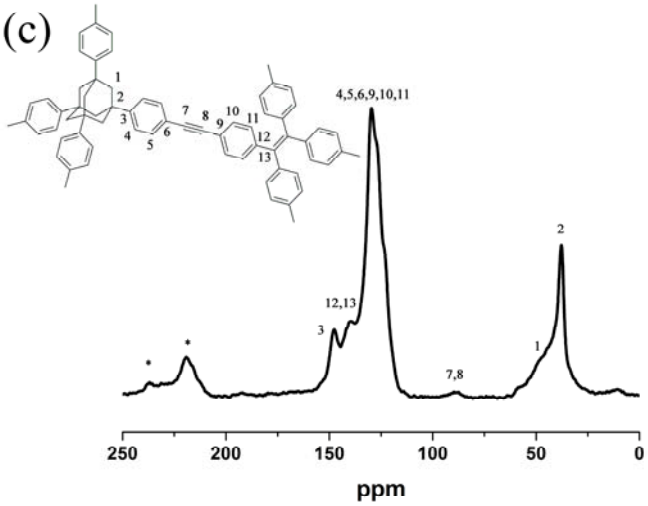
4,5,6,9,10,11
12,13
3
7,8
1
2
250
200
150
100
50
0
ppm

(d)

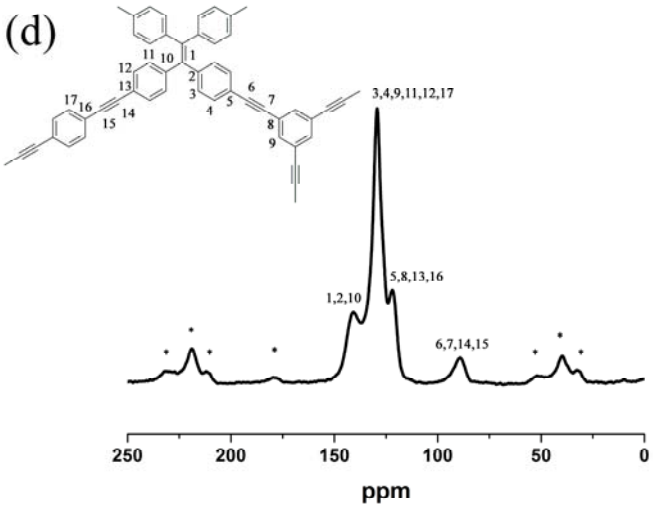
3,4,9,11,12,17
5,8,13,16
1,2,10
6,7,14,15
250
200
150
100
50
0
ppm

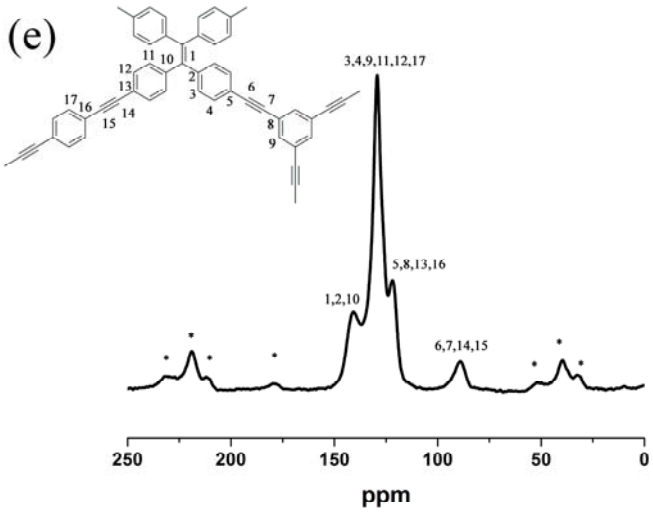

Figure IV-1. ^{13}C CP/MAS NMR spectra of (a) TPE-DB, (b) TPE-TB, (c) TPE-AD, (d) TPE-DB/TB(1:2), and (e)TPE-DB/TB(3:2). The asterisk marks a rotational sideband.

The SEM images of TPE-DB, TPE-TB, and TPE-AD showed aggregated polymer particles with sizes of about 40 – 60 nm [Figure IV-2(a)-(c)]. TPE-DB and TPE-TB were expected to have 2-dimensional structures because of the planarity of their monomers, but no crystalline reflections were observed in the wide angle X-ray diffraction patterns of all polymers [Figure IV-3(a)]. TPE-DB/TB(1:2) and TPE-DB/TB(3:2) showed similar morphologies to TPE-DB and TPE-TB. Polymeric aggregates with sizes of about 30 – 50 nm were

observed by SEM [Figure IV-2(d)-(e)]. The WXRD patterns of the polymers also indicated that the polymers have the amorphous structures [Figure IV-3(b)].

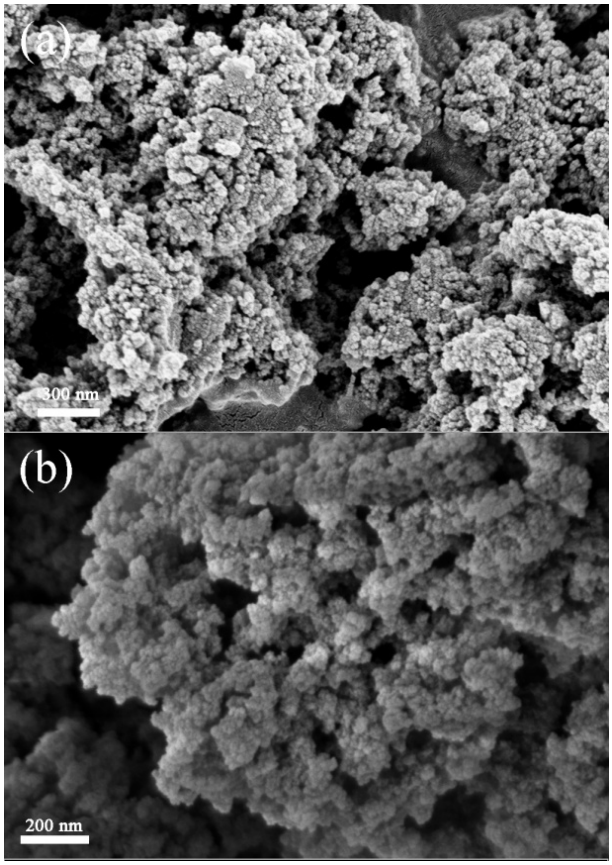

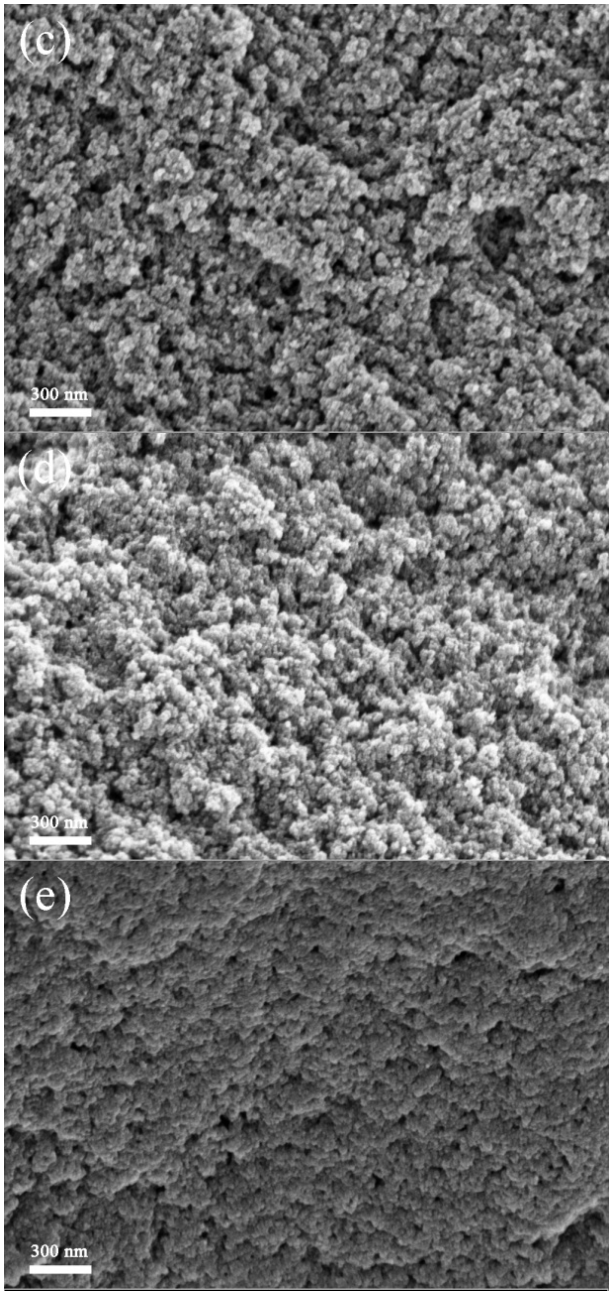

Figure IV-2. SEM images of (a) TPE-DB, (b) TPE-TB, (c) TPE-AD, (d) TPE-DB/TB(1:2), and (e) TPE-DB/TB(3:2).

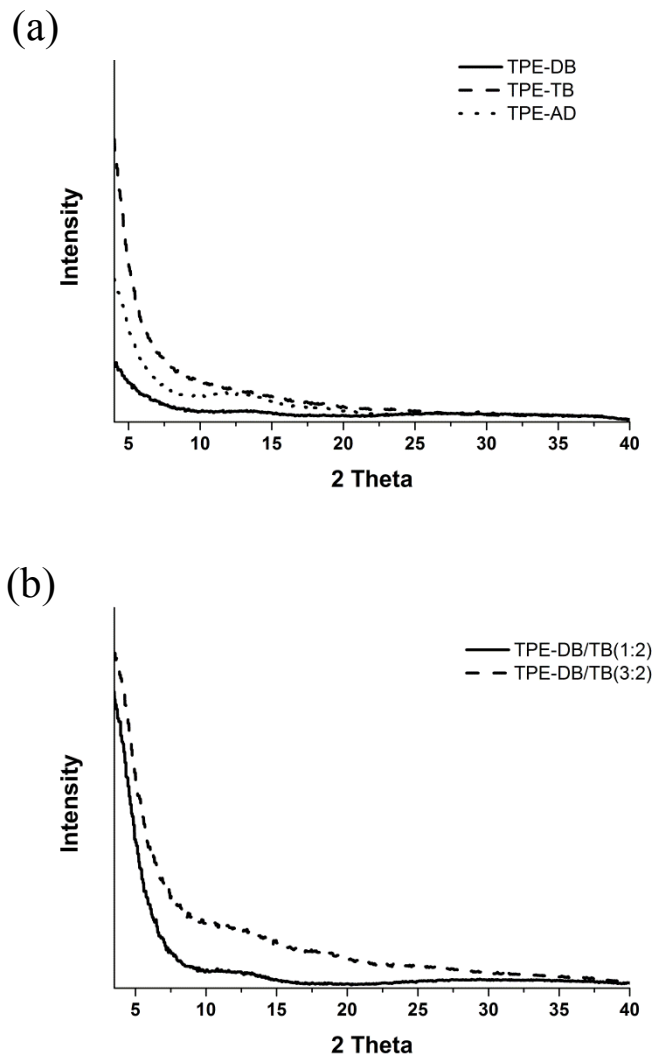

Figure IV-3. WXRD patterns of the polymers: (a) TPE-DB, TPE-TB, and TPE-AD; (b) TPE-DB/TB(1:2) and TPE-DB/TB(3:2).

The pore structures of the polymers were investigated by a cryogenic N_2adsorption-desorption experiment [Figure IV-4]. The isotherms of TPE-TB

and TPE-AD exhibited hysteresis loops of type H4 according to IUPAC classifications, indicating the swelling of polymer networks by N_2.[128] The Brunauer-Emmett-Teller (BET) surface areas of the polymers were obtained from the N_2 adsorption isotherms at 77 K. Among the polymers with one type of ethynyl units, TPE-TB showed the highest BET surface area of 1230 m^2/g, followed by TPE-DB (404 m^2/g) and TPE-AD (615 m^2/g). The pore size distributions of the polymers calculated based on nonlocal density functional theory (NLDFT) showed the presence of micropores and mesopores. The dominant pore diameters of TPE-DB, TPE-TB, and TPE-AD were 0.73, 0.78 and 1.30 nm, respectively.

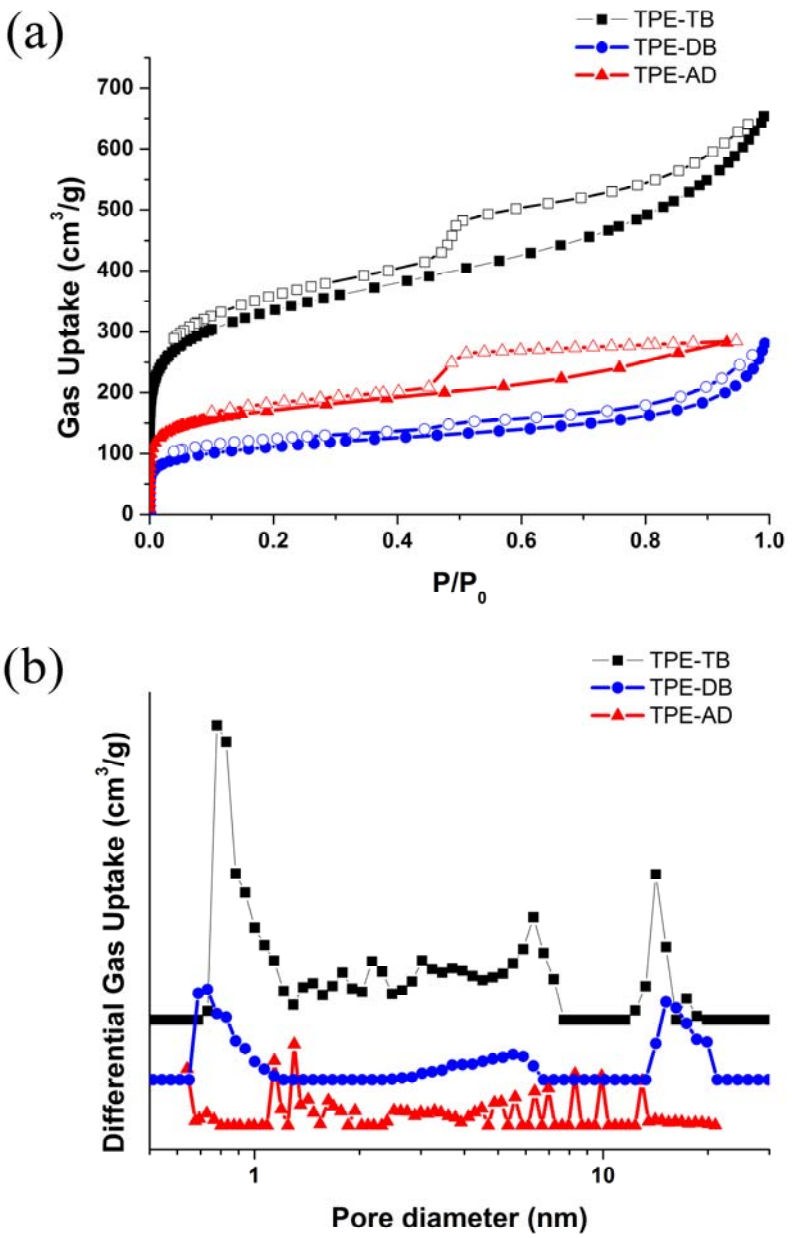

Figure IV-4. (a) Nitrogen adsorption-desorption isotherms and (b) NLDFT pore size distributions of TPE-DB, TPE-TB, and TPE-AD.

The pore structures could be changed by introducing the second ethynyl units into the polymers. Figure III-5 shows nitrogen adsorption-desorption isotherms and NLDFT pore size distributions of TPE-DB/TB(1:2) and TPE-DB/TB(3:2) obtained by using a mixture of 1,4-diethynylbenzene and 1,3,5-triethynylbenzene in molar ratios of 1 : 2 and 3 : 2, respectively, for the coupling reaction with TIPE. Notably, TPE-DB/TB(3:2) exhibited a significantly enhanced BET surface area of 1830 m^2/g compared with TPE-DB and TPE-TB. TPE-DB/TB(1:2) had a higher BET surface area than TPE-DB but a lower than TPE-TB. A type H4 hysteresis loop was observed on its isotherms. The dominant pore diameters of TPE-DB/TB(1:2) and TPE-DB/TB(3:2) were 1.40 and 0.69 nm, respectively.

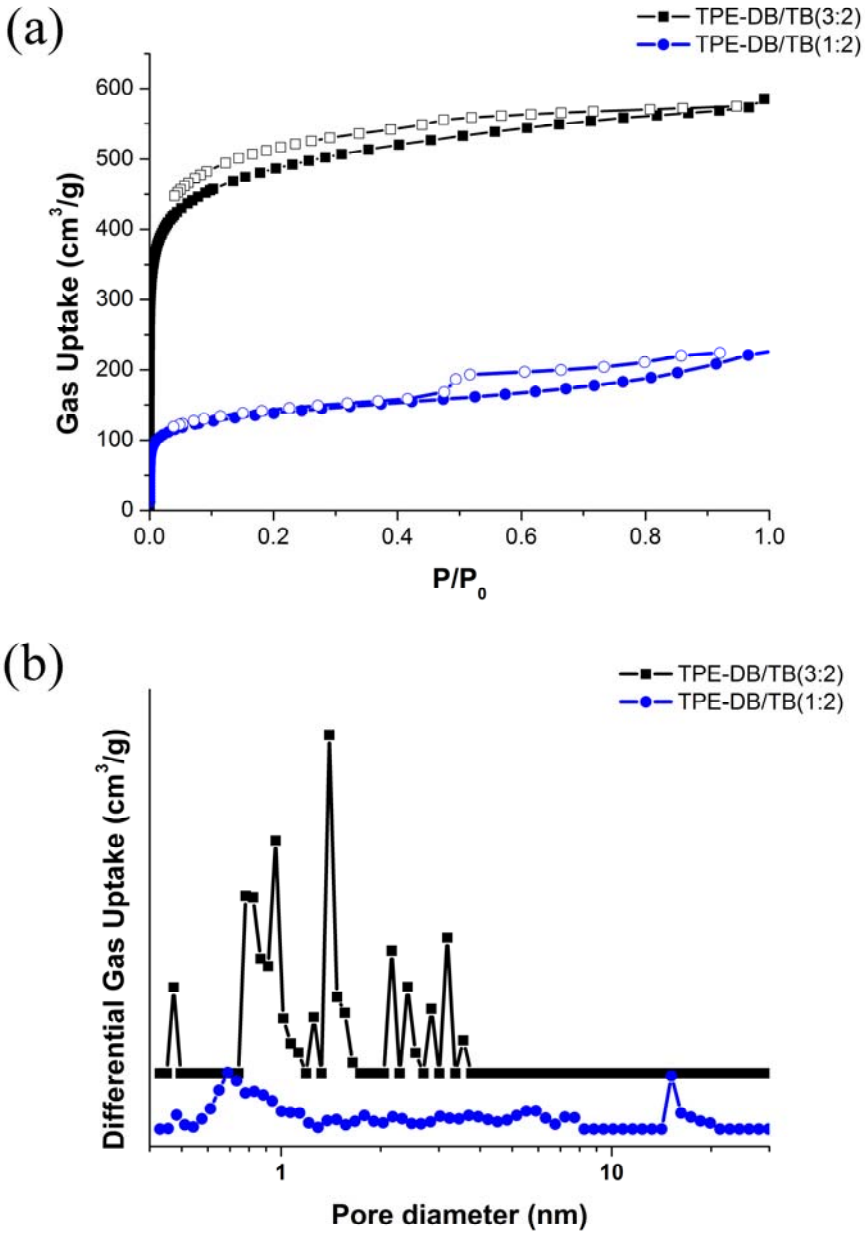

Figure IV-5. (a) Nitrogen adsorption-desorption isotherms and (b) NLDFT pore size distributions of TPE-DB/TB(1:2) and TPE-DB/TB(3:2).

Figure IV-6 shows the CO_2 and H_2 adsorption isotherms measured up to 1 bar at 273 K and 77 K, respectively. The polymers except TPE-DB showed CO_2 and H_2 uptakes over 40 and 100 cm^3/g, respectively. TPE-TB showed the highest H_2 uptake of 1.29 wt.%, which was comparable with other microporous polymers having similar surface areas such as the PI-1 (1407 m^2/g, 1.33 wt.% at 1 bar),[129] $P(1,4\text{-DEB})_N$ (809 m^2/g, 0.69 wt.% at 1 bar),[130] and BLP-2(Cl) (1174 m^2/g, 1.30 wt.% at 1 bar).[131] The BET surface areas, total pore volumes, CO_2, and H_2 adsorption properties of the polymers are summarized in Table IV-1.

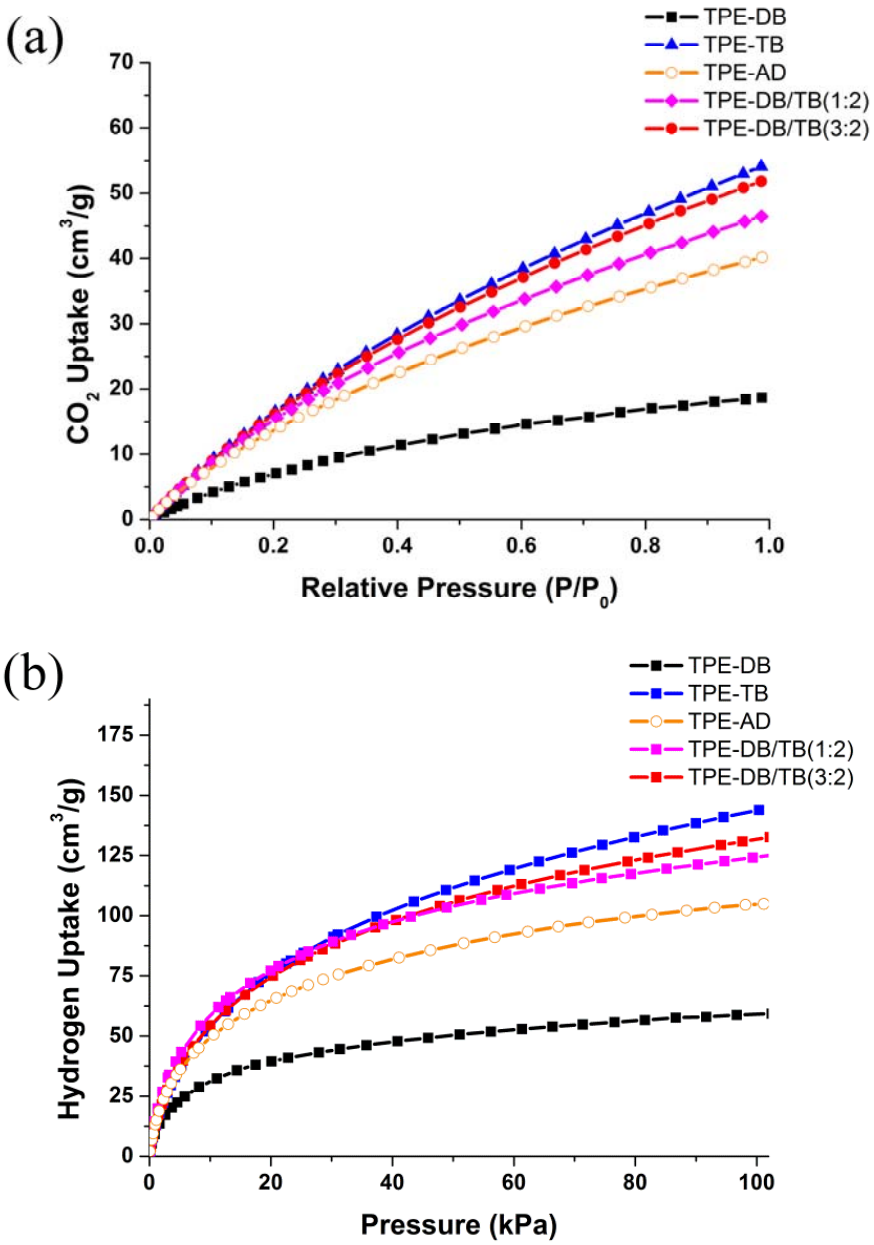

Figure IV-6. (a) CO_2 (273 K) and (b) H_2 (77 K) uptake behaviors of the polymers.

Table IV-1. Porosity Properties and Gas Uptake Capacities of the Microporous Polymers.

Polymers	BET surface area (m^2/g)	Total pore volume (cm^3/g)	CO_2 uptake at 273 K (cm^3/g)	H_2 uptake at 77 K (wt.%)
TPE-DB	404	0.434	18.6	0.529
TPE-TB	1230	1.01	54.0	1.28
TPE-AD	615	0.440	40.1	0.937
TPE-DB/TB(1:2)	513	0.349	46.4	1.12
TPE-DB/TB(3:2)	1830	0.905	51.8	1.18

IV-4. Conclusion

Microporous polymers were prepared by Sonogashira-Hagihara cross-coupling reaction of TIPE with ethynylbenzene derivatives. The BET surface areas of the polymers were dependent on the structures of the ethynylbenzenes. When two different ethynyl compounds were used for the coupling reaction, the porosity of the resulting polymer was also influenced by their molar ratio. The polymer prepared by using 1,4-diethynylbenzene and 1,3,5-triethynylbenzene in a molar ratio of 3 : 2 showed a significantly enhanced BET surface area.

Chapter V. Preparation of Microporous Polymers by Heck Cross-Coupling Reaction with a PCP Pincer Catalyst

V-1. Introduction

In 1968, Heck reported the alkenylation of benzene derivatives by the reaction of an aryl iodide with an alkene using Pd on carbon or $Pd(OAc)_2$ as a catalyst.[132,133] The reaction is certainly a useful and versatile method of carbon–carbon bond formation involving sp^2 carbons. Heck cross-coupling reaction consists of three elemental reactions: (1) oxidative addition of an organic halide to form the arylpalladium halide, (2) insertion of an alkene to form the alkyl palladium and (3) dehydropalladation to give the arylalkenes.

Only a few examples of microporous organic polymers have been prepared by Heck cross coupling reaction. Sun et al. reported luminescent MOPs obtained from aromatic halides and 1,3,5-tri(4-ethenylphenyl)benzene by Heck cross-coupling reaction.[134] The emissions of the luminescent MOPs could be quenched by picric acid, suggesting that they could serve as a sensor.

In this study, microporous polymers were prepared by Heck cross-coupling reaction with a PCP pincer catalyst. The palladium PCP pincer complexes are known to have an extraordinarily catalytic activity for the Heck couplings with halo-arenes.

V-2. Experimental

Materials. 1,3,5-Trichlorobenzene, 1,3,5-(4-bromophenyl)benzene, divinylbenzene, palladium(II) chloride, 1,5-cyclooctadiene, DMAP, resorcinol, cesium acetate and diisopropylchlorophosphine (ClP^iPr_2) were purchased from Aldrich and used as received. Other reagent-grade solvents were used as received.

Measurements. ^1H nuclear magnetic resonance (NMR) spectra were measured by a Bruker Avance DPX-300 (300 MHz) spectrometer. All chemical shifts were listed in ppm downfield from tetramethylsilane (^1H NMR).^{13}C Solid state NMR measurements were carried out on a Bruker 400 Solid/Micro-Imaging High Resolution NMR with resonance frequencies of 100 MHz. Fourier transform infrared (FT-IR) measurements were recorded on a PERKIN ELMER Spectrum GX I using KBr pellets. N_2, H_2, and CO_2 uptake amounts were measured by using a Belsorp-Max (BEL Japan, Inc.) apparatus. Ultra-high purity grade N_2, H_2, and CO_2 were used for all adsorption measurements. Field Emission Scanning Electron Microsope image was obtained by using a JSM-6700F.

Synthesis of Dichloro(1,5-cyclooctadiene)palladium(II). The synthesis of dichloro(1,5-cyclooctadiene)palladium(II) ($Pd(COD)Cl_2$) was followed according to the reported procedure.[135] Palladium(II) chloride (1.0 g, 5.65 mmol) was dissolved in concentrated HCl (5 mL). The solution was diluted with ethanol (150 mL). The solution was filtered and washed with ethanol twice. The 1,5-cyclooctadiene (3 mL) was added into the filtrate. The yellow precipitate was shown immediately. After 10 min, the compound was filtered and washed with diethylether. Yield: 1.3 g. FT-IR (KBr pellet): 2988, 2933, 2881, 1515, 1476, 1422, 1340, 1238, 1177, 1085, 995, 906, 864, 790, 678.

Synthesis of C_6H_4-2,6-$(OP^iPr_2)_2$. The synthesis of C_6H_4-2,6-$(OP^iPr_2)_2$ was followed according to reported procedure.[136,137] To a solution of resorcinol (0.36 g, 3.28 mmol) and DMAP (0.81 g, 6.60 mmol) in THF (30 ml), the ClP^iPr_2 (1.0 g, 6.55 mmol) solution in THF (20 ml) was added, while stirring at 0°C. The solution was allowed to reach room temperature and stirred for an additional 24 h. After evaporation of the solvent, the solid residue was dissolved in toluene and washed with water. The organic phase was filtered through a short plug of Celite and dried in vacuum to yield the product as a colorless oil. Yield: 1.1g (95 %). ^1H NMR (300 MHz, $CDCl_3$): δ 7.10–6.80 (m, 4H, ArH), 2.00–1.80 (m, 4H,CH), 1.15–1.00 (m, 24H, $CH(CH_3)_2$).

Synthesis of PdCl{C_6H_3-2,6-(OP^iPr_2)}. To a solution of C_6H_4-2,6-(OP^iPr_2)$_2$ (500 mg, 1.46 mmol) in toluene (50 mL), $PdCl_2$(COD) (417 mg, 1.46 mmol) was added at room temperature. The solution was refluxed for 5 h. After evaporation of the solvent, the crude product was dissolved in *n*-hexane and washed with water. The organic phase was dried by anhydrous magnesium sulfate. After filtration, the solvent was evaporated and the product was isolated by recrytallization from diethylether. Yield: 630 mg, (90 %). ^{1}H NMR (300 MHz, $CDCl_3$): δ 1.20–1.40 (m, 24H, $CH(CH_3)_2$), 2.40–2.52 (sep m, 4H, CH), 6.54 (d, 2H, ArH), 6.96 (t, 1H, ArH).

Preparation of MP-H1. To a solution of dibinylbenzene (0.250 mL, 1.74 mmol) and 1,3,5-trichlorobenzene (0.210 g, 1.16 mmol) in DMF (80 mL), PdCl{C_6H_3 -2,6 -($OPPri_2$)} (8.40 mg, 0.174 mmol) and cesium acetate (0.734 g, 3.82 mmol) were added at room temperature. The solution was stirred at 130 ^oC for 2 days. The precipitated polymer was isolated by filtration and washed with THF, dichloromethane, methanol, and water. The polymer was further purified by soxhlet-extraction with methanol for 12 h and dried in vacuum. Yield: 0.155 g. FT-IR (KBr pellet): 3085, 3052, 3022, 1604, 1501, 1448, 1362, 989, 904, 835, 793, 710.

Preparation of MP-H2. The polymer was prepared in the same manner as the preparation of MP-H1. From dibinylbenzene (0.250 mL, 1.74 mmol) and 1,3,5-tribromophenylbenzene (0.635 g, 1.16 mmol), 0.342 g of the polymer was obtained. FT-IR (KBr pellet): 3020, 1591, 1508, 1436, 1392, 956, 812, 726, 686.

Preparation of Carbonized Polymers (MP-H2C). Carbonized polymer MP-H2C was prepared as the following procedure. The temperature was elevated to 400 ^{o}C under the nitrogen atmosphere. The heating rate was 10 ^{o}C/min. After the isothermal process for 60 minutes at 400 ^{o}C, the temperature was elevated to 800°C with the same heating rate. Another isothermal process was done for 60 minute at 800°C. Char yield of MP-H2C was 71.1 wt.%.

V-3. Results and Discussion

The synthesis of the PCP catalyst was performed according to Scheme V-1. The ligand precursor 1,3-bis(diisopropylphosphinito)benzene was prepared in a 95% yield from the reaction of chlorodiisopropylphosphine and resorcinol in the presence of DMAP in THF at 25°C. $Pd(COD)Cl_2$ was synthesized according to the previous report.[135] Refluxing the bis(phosphinito)benzene with $Pd(COD)Cl_2$ in toluene for 5 h yielded the palladium complex $PdCl\{C_6H_3\text{-}2,6\text{-}(OP^iPr_2)_2\}$. The product was isolated in 90% yield as a white powder upon recrystalization from diethyl ether. The complex was highly stable to atmospheric oxygen and moisture.

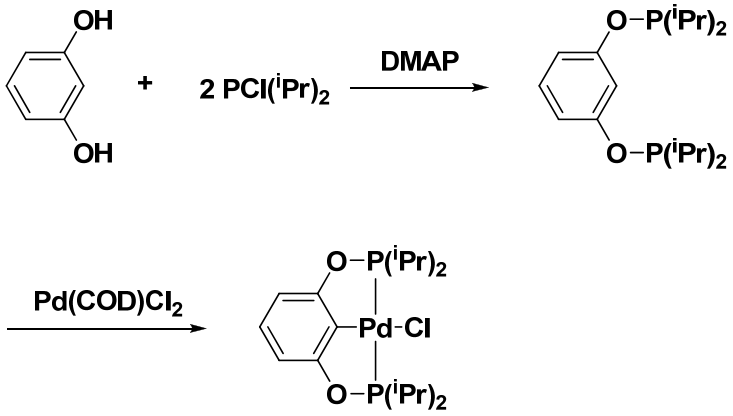

Scheme V-1. Synthesis of the PCP catalyst.

The preparation of microporous polymers was carried out according to Scheme V-2. First, arylhalides were dissolved in dry DMF and then the PCP pincer catalyst, cesium acetate, and divinylbenzene were added into the solution. The mixture was stirred at 130°C for 2 days. MP-H1 and MP-H2 were synthesized from 1,3,5-trichlorobenzene and 1,3,5-tri(4-bromophenyl)benzene, respectively. The insoluble polymers were filtered and washed with water, methanol, dichloromethane, and THF in order to remove the inorganic salts, organic monomers, and oligomers.

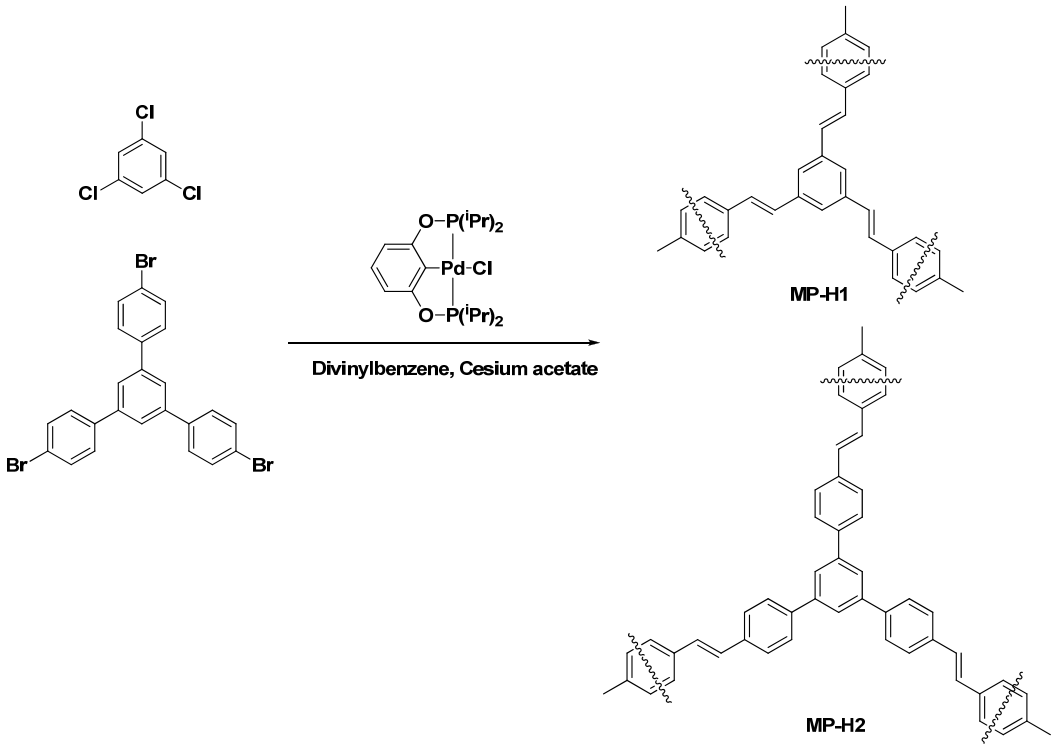

Scheme V-2. Preparation of MP-H1 and MP-H2.

The scanning electron microscopy (SEM) images of MP-H1 and MP-H2 are shown in Figure V-1. The MP-H1 had a sponge-like morphlogy. The MP-H2 had spherical aggregates with a size of 2 – 6 μm.

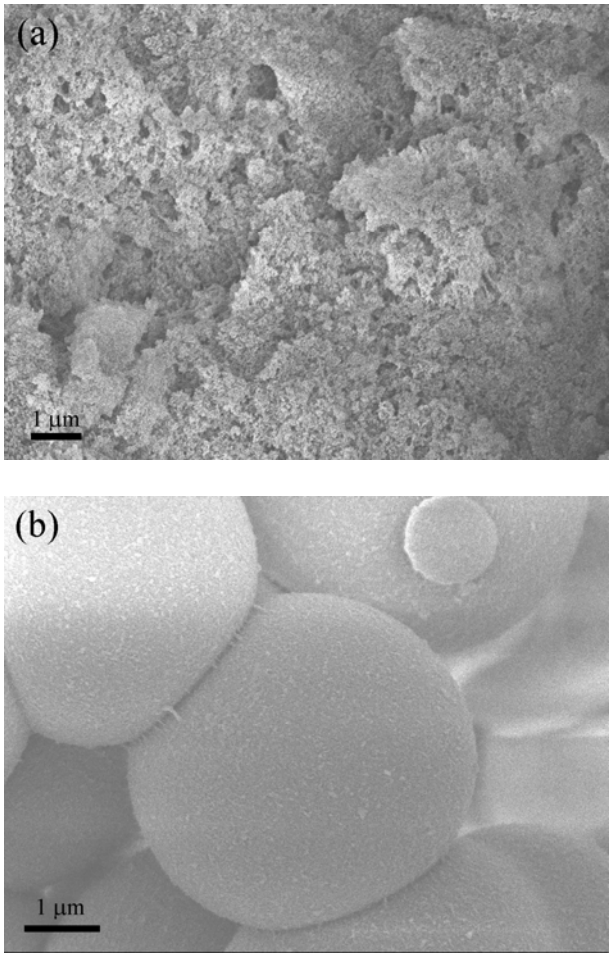

Figure V-1. SEM images of (a) MP-H1 and (b) MP-H2.

The structures of MP-H1 and MP-H2 were investigated by ^{13}C CP/MAS NMR spectroscopy [Figure V-2]. MP-H1 and MP-H2 showed peaks at 123-145 ppm, corresponding to the aromatic carbons. The peaks of vinyl carbons overlapped with those of the aromatic carbons.

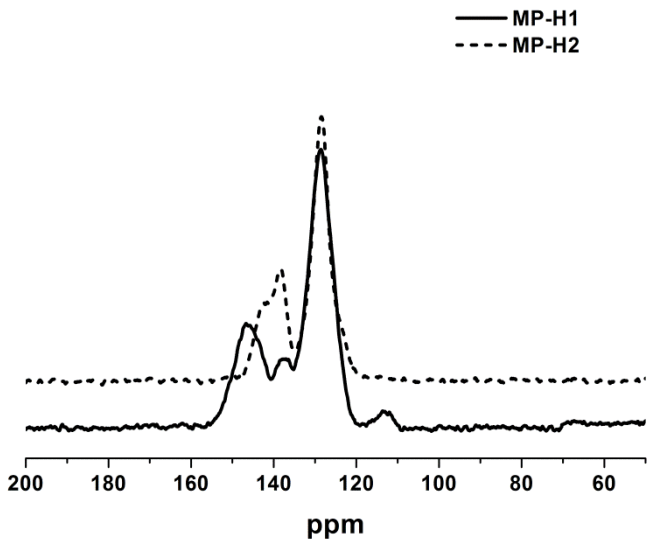

Figure V-2. ^{13}C CP/MAS NMR spectra of MP-H1 and MP-H2.

The porous properties of the MP-H1 and MP-H2 were investigated by N_2 adsorption-desorption analysis at 77 K [Figure V-3]. According to the IUPAC classification, MP-H1 exhibited a Type II adsorption isotherm. A high uptake of N_2 at low pressure, observed from the N_2 adsorption isotherm of MP-H1, indicated that MP-H1 had mainly micro- and mesopores. The BET surface

areas of MP-H1 and MP-H2 were 767 and 3.40 m^2/g, respectively.

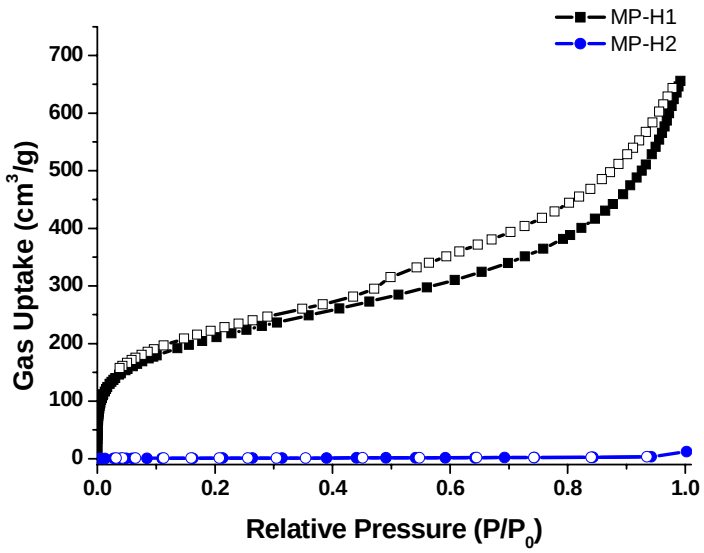

Figure V-3. N_2 adsorption-desorption isotherms of MP-H1 and MP-H2 at 77K.

MP-H2 was carbonized and the surface area change was investigated [Figure V-4]. The carbonized polymer MP-H2C showed a significant increase of the surface area. The carbonized MP-H2 (MP-H2C) showed a type I isotherm, which indicated that it was microporous. The BET surface area of MP-H2C was 856 m^2/g. The NLDFT pore size distribution of MP-H2C showed that the dorminant pore size was 0.45 nm [Figure V-4(b)].

The CO_2 adsorption amounts of MP-H2C at 1 atm were 113 cm^3/g (5.04

mmol/g) and 82.4 cm^3/g (3.68 mmol/g) at 273 and 298 K, respectively [Figure V-5]. These uptakes were relatively high compared with other microporous polymer, such as PAF-1 (2.07 mmol/g at 273 K),[138] 1,3,5-triphenylbenzene HCP (3.61 mmol/g at 273 K),[71] and BILP-1 (4.3 mmol/g at 273 K).[52] At zero coverage, the isosteric heat of adsorption (Qst) value was 29.1 kJ/mol [Figure V-6].

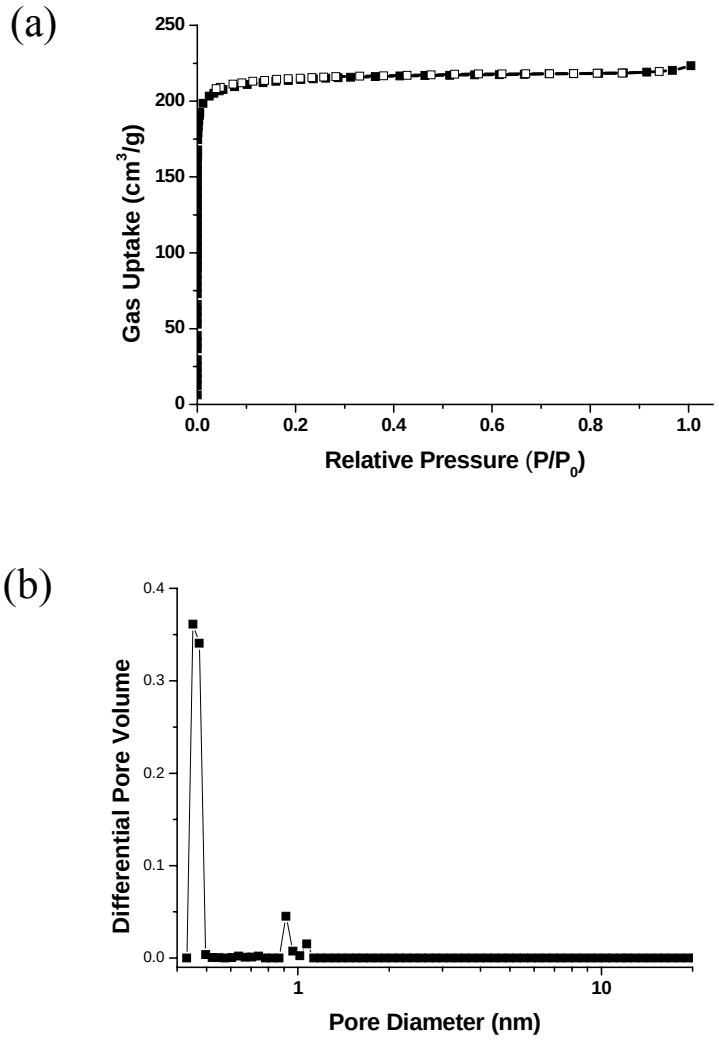

Figure V-4. (a) N_2 adsorption-desorption isotherms at 77 K and (b) NLDFT pore size distribution of MP-H2C.

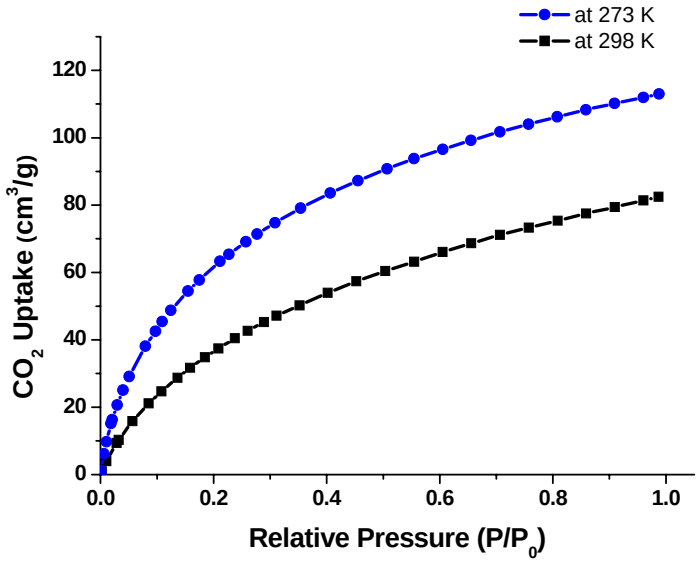

Figure V-5. CO_2 adsorption isotherms of MP-H2C at 273 and 298 K.

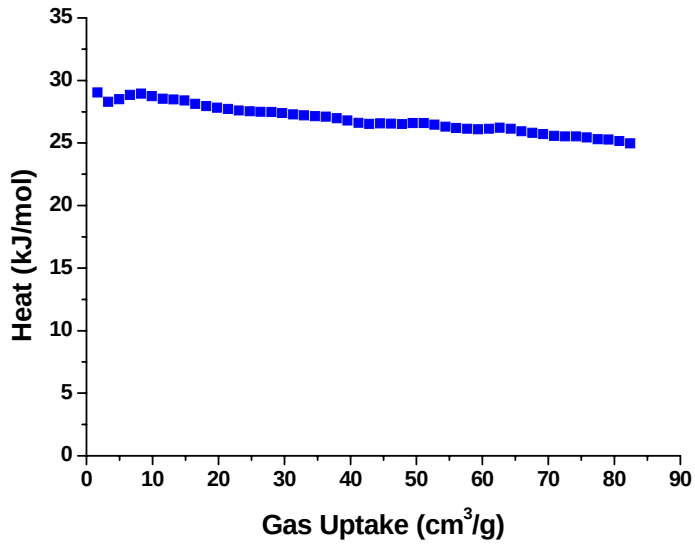

Figure V-6. CO_2 heat of adsorption of MP-H2C.

The H_2 adsorption of MP-H2C measured at 77 K and 1 bar was 175.3 cm^3/g (1.57 wt.%) [Figure V-7]. This value was relatively high with other microporous polymers that have similar surface areas like PI-1 (1407 m^2/g, 1.33 wt.% at 1 bar),[129] $P(1,4\text{-DEB})_N$ (809 m^2/g, 0.69 wt.% at 1 bar),[130] and BLP-2(Cl) (1174 m^2/g, 1.30 wt.% at 1 bar).[131] The high H_2 uptake of MP-H2C was likely due to the presence of ultramicropores with a size of below 1 nm [Figure V-4(b)].

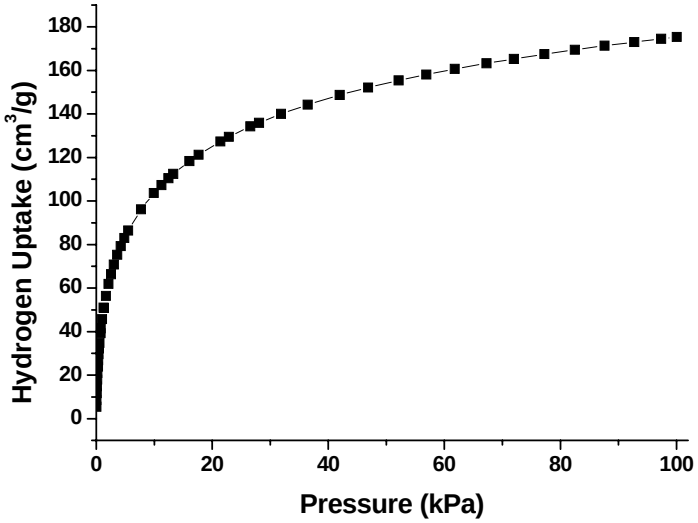

Figure V-7. H_2 uptake of MP-H2C.

V-4 Conclusion

In conclusion, microporous polymers, MP-H1 and MP-H2, were prepared by Heck cross-coupling reaction with the PCP pincer catalyst. The synthesized PCP pincer catalyst was highly efficient for Heck cross-coupling reaction. The MP-H2 had a small BET surface area, but after carbonization, the BET surface area increased significantly. MP-H2C showed a type I isotherm and a BET surface area of 856 m^2/g. MP-H2C also had high gas adsorption properties.

Chapter VI. References

(1) Rouquerol, J.; Avnir, D.; Fairbridge, C. W.; Everett, D. H.; Haynes, J. M.; Pernicone, N.; Ramsay, J. D. F.; Sing K. S. W.; Unger, K. K. *Pure & Appl. Chem* **1994**, *66*, 1739–1758.

(2) Langmuir, I. *J. Amer. Chem. Soc*. **1918**, *40*, 1361–1403.

(3) Brunauer , S.; Emmett , P. H.; Teller, E. *J. Am. Chem. Soc*. **1938**, *60*, 309–319.

(4) Horvath, G.; Kawazoe, K. *J. Chem. Eng. Jpn*. **1983**, 16, 470–475.

(5) Saito A.; Foley H. C. *Amer. Inst. Chem. Eng. J*. **1991**,*37*, 429–436.

(6) Saito A.; Foley H. C *Microporous Materials* **1995**, *3*, 531–542.

(7) Cheng, L.S.; Yang, R. T. *Chem. Eng. Sci.* **1994**, *49*, 2599–2609.

(8) Barrett, E. P.; Joyner, L. G.; Halenda, P. P. *J. Am. Chem. Soc.* **1951**, *73*, 373–380.

(9) Seaton, N. A.; Walton, J. P. R. B.; Quirke, N. *Carbon* **1989**, *27*, 853–861.

(10) Ravikovitch, P. I.; Vishnyakov, A.; Russo, R.; Neimark A. V. *Langmuir* **2000**, *16*, 2311–2320.

(11) Jagiello, J.; Thommes, M. *Carbon* **2004**, *42*, 1227–1232.

(12) Rosi, N. L.; Eckert, J.; Eddaoudi, M.; Vodak, D. V.; Kim, J.;

O'Keeffe, M.; Yaghi, O. M. *Science* **2003**, *300*, 1127–1129.

(13) Furukawa, H.; Ko, N.; Go, Y. B.; Aratani, N.; Choi, S. B.; Choi, E.; Yazaydin, A. O.; Snurr, R. Q.; O'Keeffe, M.; Kim, J.; Yaghi, O. M. *Science* **2010**, *329*, 424–428.

(14) Nguyen, J. G.; Cohen, S. M. *J. Am. Chem. Soc.* **2010**, *132*, 4560–4561.

(15) Demessence, A.; D'Alessandro, D. M.; Foo, M. L.; Long, J. R. *J. Am. Chem. Soc.* **2009**, *131*, 8784–8786.

(16) Rowsell, J. L. C.; Yaghi, O. M. *J. Am. Chem. Soc.* **2006**, *128*, 1304–1315.

(17) Rowsell, J. L. C.; Millward, A. R.; Park, K. S.; Yaghi, O. M. *J. Am. Chem. Soc.* **2004**, *126*, 5666–5667.

(18) Férey, G.; Latroche, M.; Serre, C.; Millange, F.; Loiseaua, T.; Percheron-Guéganb, A. *Chem. Commun.* **2003**, *39*, 2976–2977.

(19) Latroche, C.; Surbl, S.; Serre, C.; Mellot-Draznieks, C.; Llewellyn, P. L.; Lee, J. -H.; Chang, J. S.; Jhung, S. H.; Fèrey, G. *Angew. Chem. Int. Ed.* **2006**, *45*, 8227 –8231.

(20) Surblè, S.; Millange, F.; Serre, C.; Düren, T.; Latroche, L.; Bourrelly, S.; Llewellyn, P. L.; Fèrey, G. *J. Am. Chem. Soc.* **2006**, *128*, 14889–14896.

(21) Côtè, A. P.; Benin, A. I.; Ockwig, N. W.; O'Keeffe, M.; Matzger, A. J.; Yaghi, O. M. *Science* **2005**, *310*, 1166–1170.

(22) El-Kaderi, H. M.; Hunt, J. R.; Mendoza-Cortés, J. L.; Côté, A. P.; Taylor, R. E.; O'Keeffe, M.; Yaghi, O. M. *Science* **2007**, *316*, 268–272.

(23) Côtè, A. P.; El-Kaderi, H. M.; Furukawa, H.; Hunt, J. R.; Yaghi, O. M. *J. Am. Chem. Soc.* **2007**, *129*, 12914–12915.

(24) Wan, S.; Guo, J.; Kim, J.; Ihee, H.; Jiang, D. . *Angew. Chem. Int. Ed.* **2008**, *120*, 8958 –8962.

(25) Tilford, R. W.; Mugavero III, S. J.; Pellechia, S. J.; Lavigne J. J. *Adv. Mater.* **2008**, *20*, 2741–2746.

(26) Han, S. S.; Furukawa, H.; Yaghi, O. M.; Goddard III, W. A. J. Am. Chem. Soc. **2008**, *130*, 11580–11581.

(27) Wan, S.; Guo, J.; Kim, J.; Ihee, H.; Jiang, D. *Angew. Chem. Int. Ed.* **2009**, *48*, 5439 –5442.

(28) Furukawa, H.; Yaghi, O. M. *J. Am. Chem. Soc.* **2009**, *131*, 8875–8883.

(29) Spitler, E. L.; Koo, B. T.; Novotney, J. L.; Colson, J. W.; Uribe-Romo, F. J.; Gutierrez, G. D.; Clancy, P.; Dichtel, W. R. *J. Am. Chem. Soc.* **2011**, *133*, 19416–19421.

(30) Budd, P. M.; Ghanem, B. S.; Makhseed, S.; McKeown, N. B.;

Msayib, K. J.; Tattershall, C. E. *Chem. Commun.* **2004**, *40*, 230–231.

(31) McKeown, N. B.; Gahnem, B.; Msayib, K. J.; Budd, P. M.; Tattershall, C. E.; Mahmood, K.; Tan, S.; Book, D.; Langmi, H. W.; Walton, A. *Angew. Chem. Int. Ed.* **2006**, *45*, 1804–1807.

(32) Ghanem, B. S.; Msayib, K. J.; McKeown, N. B.; Harris, K. D. M.; Pan, Z.; Budd, P. M.; Butler, A.; Selbie, J.; Book, D.; Walton, A. *Chem. Commun.* **2007**, *43*, 67–69.

(33) Germain, J.; Hradil, J.; Frèchet, J. M. J.; Svec, F. *Chem. Mater.* **2006**, *18*, 4430–4435.

(34) Lee, J.-Y.; Wood, C. D.; Bradshaw, D.; Rosseinsky, M. J.; Cooper, A. I. *Chem. Commun.* **2006**, *42*, 2670–2672.

(35) Jiang, J.-X.; Su, F.; Trewin, A.; Wood, C. D.; Campbell, N. L.; Niu, H.; Dickinson, C. ; Ganin, A. Y.; Rosseinsky, M. J.; Khimyak Y. Z.; Cooper, A. I. *Angew. Chem., Int. Ed.,* **2007**, *46*, 8574–8578.

(36) Jiang, J.-X.; Su, F.; Trewin, A.; Wood, C. D.; Niu, H.; Jones, J. T. A.; Khimyak, Y. Z.; Cooper, A. I. *J. Am. Chem. Soc.* **2008**, *130*, 7710–7720.

(37) Dawson, R.; Laybourn, A.; Clowes, R.; Khimyak, Y. Z.; Adams, D. J.; Cooper, A. I. *Macromolecules* **2009**, *42*, 8809–8816.

(38) Jiang, J.-X.; Trewin, A.; Su, F.; Wood, C. D.; Niu, H.; Jones, J. T. A.;

Khimyak, Y. Z.; Cooper, A. I. *Macromolecules* **2009**, *42*, 2658–2666.

(39) Cooper, A. I. *Adv. Mater.* **2009**, *21*, 1291–1295.

(40) Morisaki, Y.; Gon, M.; Tsuji, Y.; Kajiwara, Y.; Chujo, Y. *Macromol. Chem. Phys.* **2012**, *213*, 572−579.

(41) Dawson, R.; Laybourn, A.; Khimyak, Y. Z.; Adams, D. J.; Cooper, A. I. *Macromolecules* **2010**, *43*, 8524–8530.

(42) Chen, L.; Yang, Y.; Jiang, D. *J. Am. Chem. Soc.* **2010**, *132*, 9138–9143.

(43) Zhang, K.; Kopetzki, D.; Seeberger, P. H.; Antonietti, M.; Vilela, F. *Angew. Chem. Int. Ed.* **2013**, *52*, 1432 –1436.

(44) Hasell, T.; Wood, C. D.; Clowes, R.; Jones, J. T. A.; Khimyak, Y. Z.; Adams, D. J.; Cooper, A. I. *Chem. Mater.* **2010**, *22*, 557–564.

(45) Zhang, P.; Weng, Z.; Guo, J.; Wang, C. *Chem. Mater.* **2011**, *23*, 5243–5249.

(46) Zhang, Y.; Zhang, Y.; Sun, Y. L.; Du, X.; Shi, J. Y.; Wang, W. D.; Wang W. *Chem. Eur. J.* **2012**, *18*, 6328 – 6334.

(47) Ben, T.; Ren, H.; Ma, S.; Cao, D.; Lan, J.; Jing, X.; Wang, W.; Xu, J.; Deng, F.; Simmons, J. M.; Qiu, S.; Zhu, G. *Angew. Chem. Int. Ed.* **2009**, *48*, 9457–9460.

(48) Schwab, M. G.; Fassbender, B.; Spiess, H. W.; Thomas, A.; Feng, X.;

Müllen, K. *J. Am. Chem. Soc*. **2009**, *131*, 7216–7217.

(49) Uribe-Romo, F. J.; Doonan, C. J.; Furukawa, H.; Oisaki, K.; Yaghi O. M. *J. Am. Chem. Soc*. **2011**, *133*, 11478–11481.

(50) Uribe-Romo, F. J.; Hunt, J. R.; Furukawa, H.; Klöck, C.; O'Keeffe, M.; Yaghi, O. M. *J. Am. Chem. Soc*. **2009**, *131*, 4570–4571.

(51) Pandey, P.; Katsoulidis, A. P.; Eryazici, I.; Wu, Y.; Kanatzidis, M. G.; Nguyen, S. T. *Chem. Mater.* **2010**, *22*, 4974–4979.

(52) Rabbani M. G.; El-Kaderi, H. M. *Chem. Mater*. **2011**, *23*, 1650–1653.

(53) Weber, J.; Antonietti, M.; Thomas, A. *Macromolecules* **2008**, *41*, 2880–2885.

(54) Farha, O. K.; Spokoyny, A. M.; Hauser, B. G.; Bae, Y.-S.; Brown, S. E.; Snurr, R. Q.; Mirkin, C. A.; Hupp, J. T. *Chem. Mater*. **2009**, *21*, 3033–3035.

(55) Wang, Z.; Zhang, B.; Yu, H.; Sun, L.; Jiao, C.; Liu, W. *Chem. Commun*. **2010**, *46*, 7730–7732.

(56) Kuhn, P.; Antonietti, M.; Thomas, A. *Angew. Chem. Int. Ed.* **2008**, *47*, 3450–3453.

(57) Chan-Thaw, C. E.; Villa, A.; Katekomol, P.; Su, D.; Thomas, A.; Prati, L. *Nano Lett.* **2010**, *10*, 537–541.

(58) Bojdys, M. J.; Wohlgemuth, S. A.; Thomas, A.; Antonietti, M.

Macromolecules **2010**, *43*, 6639–6645.

(59) Ren, S.; Bojdys, M. J.; Dawson, R.; Laybourn, A.; Khimyak, Y. Z.; Adams, D. J.;Cooper, A. I. *Adv. Mater*. **2012**, *24*, 2357–2361.

(60) Yu, H.; Shen, C.; Tian, M.; Qu, J.; Wang, Z. *Macromolecules* **2012**, *45*, 5140−5150.

(61) Ma, L.; Wanderley, M. M.; Lin, W. *ACS Catal*. **2011**, *1*, 691–697.

(62) Xie, Z.; Wang, C.; deKrafft, K. E.; Lin, W. *J. Am. Chem. Soc*. **2011**, *133*, 2056–2059.

(63) Yamamoto, T. *Prog. Polym. Sci*. **1992**, *17*, 1153−1205.

(64) Yuan, D.; Lu, W.; Zhao, D.; Zhou, H. C. *Adv. Mater*. **2011**, *23*, 3723–3725.

(65) Sonogashira, K.; Tohda, Y.; Hagihara, N. *Tetrahedron Lett*. **1975**, *16*, 4467–4470.

(66) Takahashi, S.; Kuroyama, Y.; Sonogashira, K.; Hagihara, N. *Synthesis* **1980**, 627–630.

(67) Cooper, A. I. *Adv. Mater.* **2009**, *21*, 1–5.

(68) Holst, J. R.; Stöckel, E.; Adams, D. J.; Cooper, A. I. *Macromolecules* **2010**, *43*, 8531–8538.

(69) Tyrrell E.; Brookes, P. *Synthesis* **2003**, 469–483.

(70) Chen, L.; Honsho, Y.; Seki, S.; Jiang, D. *J. Am. Chem. Soc.* **2010**,

132, 6742–6748.

(71) Li, B.; Gong, R.; Wang, W.; Huang, X.; Zhang, W.; Li, H.; Hu, C.; Tan, B. *Macromolecules* **2011**, *44*, 2410–2414.

(72) Luo, Y.; Li, B.; Wang, W.; Wu, K.; Tan, B. *Adv. Mater*. **2012**, *24*, 5703–5707.

(73) Schwab, M. G.; Lennert, A.; Pahnke, J.; Jonschker, G.; Koch, M.; Senkovska, I.; Rehahnd, M.; Kaskel, S. *J. Mater. Chem*. **2011**, *21*, 2131–2135.

(74) Dawson, R.; Ratvijitvech, T.; Corker, M.; Laybourn, A.; Khimyak, Y. Z.; Cooper, A. I.; Adams, D. J. *Polym. Chem.* **2012**, *3*, 2034–2038.

(75) Schlapbach, L.; Zuttel, A. *Nature* **2001**, *414*, 353–358.

(76) Langmi, H.W.; McGrady, G. S. *Coord. Chem. Rev*. **2007**, *251*, 925–935.

(77) Collins, D. J.; Zhou, H. C. *J. Mater. Chem.* **2007**, *17*, 3154–3160.

(78) Panella, B.; Hirscher, M.; Roth, S. *Carbon* **2005**, *43*, 2209–2214.

(79) Benard, P.; Chahine, R. *Scr. Mater*. **2007**, *56*, 803–808.

(80) McKeown, N. B.; Budd, P. M. *Chem. Soc. Rev*. **2006**, *35*, 675–683.

(81) Han, S. S.; Mendoza-Cortes, J. L.; Goddard, W. A. *Chem. Soc. Rev*. **2009**, *38*, 1460–1476.

(82) Garberoglio, G. *Langmuir* **2007**, *23*, 12154–12158.

(83) Chen, L.; Yang, Y.; Guo, Z.; Jiang, D. *Adv. Mater*. **2011**, *23*, 3149–3154.

(84) Rose, M. ; Notzon, A.; Heitbaum, M.; Nickerl, G.; Paasch, S.; Brunner, E.; Glorius, F.; Kaskel, S. *Chem. Commun.* **2011**, *47*, 4814–4816.

(85) Türünç¸ O.; Meier, M. A. R. *J. Polym. Sci. Pol. Chem*. **2010**, *50*, 1689–1695.

(86) Fairbanks, B. D.; Sims, E. A.; Anseth, K. S.; Bowman, C. N. *Macromolecules* **2010**, *43*, 4113–4119.

(87) Park, H. Y.; Kloxin, C. J.; Scott, T. F.; Bowman, C. N. *Macromolecules* **2010**, *43*, 10188–10190.

(88) Shen, Y.; Ma, Y.; Li, Z. *J. Polym. Sci. Pol. Chem*. **2013**, *51*, 708–715.

(89) Chen, G.; Kumar, J.; Gregory, A.; Stenzel, M. H.; *Chem. Commun.* **2009**, *45*, 6291–6293.

(90) Konkolewicz, D.; Gray-Weale, A.; Perrierhosh, S. *J. Am. Chem. Soc.* **2009**, *131*, 18075–18077.

(91) Liu, W.; Dong, C.-M. *Macromolecules* **2010**, *43*, 8447–8455.

(92) Konkolewicz, D.; Poon, C. K.; Gray-Weale, A.; Perrier, S.; *Chem. Commun.* **2011**, *47*, 239–241.

(93) Chan, J. W.; Yu, B.; Hoyle, C. E.; Lowe, A. B. *Chem. Commun.* **2008**,

44, 4959–4961.

(94) Fairbanks, B. D.; Scott, T. F.; C. J. Kloxin, K. S. Anseth, and C. N. Bowman, Macromolecules 2009, 42, 211–217.

(95) Wei, J.; Wang, H.; Deng, Y.; Sun, Z.; Shi, L.; Tu, B.; Luqman, M.; Zhao, D. *J. Am. Chem. Soc*. **2011**, *133*, 20369–20377.

(96) Shin, H.-S.; Huh, S. *ACS Appl. Mater. Interfaces* **2012**, *4*, 6324–6331.

(97) Ramtenki, V.; Anumon, V. D.; Badiger, M. V.; Prasad, B.L.V. *Colloid Surf. A-Physicochem. Eng. Asp*. **2012**, *414*, 296–301.

(98) Wu, S.; Dzubiella, J.; Kaiser, J.; Drechsler, M.; Guo, X.; Ballauff, M.; Lu, Y.; *Angew. Chem. Int. Ed*. **2012**, *51*, 2229 –2233.

(99) Sen, I. K.; Maity, K.; Islam, S. S. *Carbohydr. Polym*. **2013**, *91*, 518–528.

(100) Abad, A.; Concepción, P.; Corma, A.; García, H. *Angew. Chem. Int. Ed*. **2005**, *44*, 4066–4069.

(101) Li, W.; Wang, A.; Liu, X.; Zhang, T. *Appl. Catal. A-Gen*. **2012**, *433–434*, 146–151.

(102) Lee, W.-S.; Zhang, R.; Akatay, M. C.; Baertsch, C. D.; Stach, E. A.; Ribeiro, F. H.; Delgass, W. N. *ACS Catal*. **2011**, *1*, 1327–1330.

(103) Ma, W.; Chen, F. *Catal. Lett*. **2013**, *143*, 84–92.

(104) Lim, H.; Chang, J. Y. *Macromolecules* **2010**, *43*, 6943–6945.

(105) Vericat, C.; Vela, M. E.; Andreasen, G.; Salvarezza, R. C.; Vázquez, L.; Martín-Gago, J. A. *Langmuir* **2001**, *17*, 4919−4924.

(106) Minozzi, M.; Monesi, A.; Nanni, D.; Spagnolo, P.; Marchetti, N.; Massi, A. *J. Org. Chem.* **2011**, *76*, 450–459.

(107) Benati, L.; Montevecchi, P. C.; Spagnolo, P.; *J. Chem. Soc. Perkin Trans. 1* **1991**, 2103–2109.

(108) Benati, L.; Capella, L.; Montevecchi P. C.; Spagnolo, P. *J. Chem. Soc. Perkin Trans. 1* **1995**, 1035–1038.

(109) Ananikov, V. P. ; Malyshev, D. A.; Beletskaya, I. P.; Aleksandrov, G. G.; Eremenko, I. L. *Adv. Synth. Catal.* **2005**, *347*, 1993–2001.

(110) Mihaly, M. ; Fleancu, M. C.; Olteanu, N. L.; Bojin, D.; Meghea, A.; Enachescu, M. *C. R. Chimie* **2012**, *15*, 1012–1021.

(111) Zotti, G.; Vercelli, B.; Berlin, A. *Chem. Mater*. **2008**, *20*, 397–412.

(112) Jiang, G.; Wang, L.; Chen, W. *Mater. Lett*. **2007**, *61*, 278–283.

(113) Si, R.; F.-Stephanopoulos, M. *Angew. Chem. Int. Ed*. **2008**, *47*, 2884 –2887.

(114) Sahu, D.; Chu, H.-C.; Yang, P.-J.; Lin, H.-C. *Macromol. Chem. Phys.* **2012**, *213*, 1550−1558.

(115) Zhao, Z.; Chen, S.; Shen, X.; Mahtab, F.; Yu, Y.; Lu, P.; Lam, J. W. Y.; Kwok, H. S.; Tang, B. Z. *Chem. Commun.* **2010**, *46*, 686–688.

(116) Komiyama, M.; Takeuchi, T.; Mukawa, T.; Asunuma, H.; Molecular imprinting from fundamentals to applications, Wiley-VCH, Weinheim, Germany, **2003**.

(117) Wulff, G.; Schauhoff, S. *J. Org. Chem.* **1991**, *56*, 395–400.

(118) Mosbach, K. *React. Funct. Polym*. **1999**, *41*, 115–124.

(119) Kim, Y.; Jeon, J. B.; Chang, J. Y. *J. Mater. Chem*. **2012**, *22*, 24075–24080.

(120) Kim, W. J.; Chang, J. Y. *Materials Letters* **2011**, *65*, 1388–1391.

(121) Stöckel, E.; Wu, X.; Trewin, A.; Wood, C. D.; Clowes, R.; Campbell, N. L.; Jones, J. T. A.; Khimyak, Y. Z.; Adams, D. J.; Cooper, A. I. *Chem. Commun*. **2009**, *45*, 212–214.

(122) Ren, S.; Dawson, R.; Laybourn, A.; Jiang, J.-X.; Khimyak, Y.; Adams, D. J.; Cooper, A. I. *Polym. Chem.* **2012**, *3*, 928–934.

(123) Dawson, R.; Adams, D. J.; Cooper, A. I. *Chem. Sci*. **2011**, *2*, 1173–1177.

(124) Sengupta, S. *Synlett.* **2004**, *7*, 1191–1194.

(125) Xu, Y.; Chen, L.; Guo, Z.; Nagai, A.; Jiang D. *J. Am. Chem. Soc.* **2011**, *133*, 17622–17625.

(126) Xu, Y.; Nagai, A.; Jiang, D., *Chem. Comm*. **2013**, *49*, 1591–1593.

(127) Lu, W.; Yuan, D.; Zhao, D.; Schilling, C. I.; Plietzsch, O.; Muller, T.;

Bräse, S.; Guenther, J.; Blümel, J.; Krishna, R.; Li, Z.; Zhou, H.-C. *Chem. Mater.* **2010**, *22*, 5964–5972.

(128) Schmidt, J.; Werner, M.; Thomas, A. *Macromolecules* **2009**, *42*, 4426–4429.

(129) Wang, Z.; Zhang, B.; Yu, H.; Sun, L.; Jiao, C.; Liua, W. *Chem. Commun.* **2010**, *46*, 7730–7732.

(130) Hanková, V.; Slováková, E.; Zedník, J.; Vohlídal, J.; Sivkova, R.; Balcar, H.; Zukal, A.; Brus, J.; Sedláček, J. *Macromol. Rapid Commun.* **2012**, *33*, 158–163.

(131) Reich, T. E.; Jackson, K. T.; Li, S.; Jena, P.; El-Kaderi, H. M.; *J. Mater. Chem.* **2011**, *21*, 10629–10632.

(132) Moritani, I.; Fujiwara, Y. *Tetrahedron Lett.* **1967**, *8*, 1119–1122.

(133) Heck, R. F. *J. Am. Chem. Soc*. **1968**, *90*, 5518–5546.

(134) Sun, L.; Liang, Z.; Yu, J.; Xu, R. *Polym. Chem.* **2013**, *4*, 1932–1938.

(135) Booth, H. S. Inorganic syntheses, Wiley, New York, **1975**.

(136) Morales-Morales, D.; Grause, C.; Kasaoka, K.; Redón, R.; Cramer, R. E.; Jensen, C. M. *Inorganica Chimica Acta* **2000**, *300–302*, 958–963.

(137) Morales-Morales, D.; Redón, R.; Yung C.; Jensen, C. M. *Chem. Commun*. **2000**, *36*, 1619–1620.

(138) Ben, T.; Pei, C.; Zhang, D.; Xu, J.; Deng, F.; Jing, X.; Qiu, S. *Energy*

Environ. Sci. **2011**, *4*, 3991–3999.

국문요약

다공성 고분자는 높은 비표면적 및 열적, 화학적 안정성으로 촉매의 담지, 물질의 저장 또는 분리에 사용될 수 있다. 이러한 다공성 고분자의 기공은 크기에 따라서 2 나노미터 이하의 마이크로포어(micropore), 2 ~ 50 나노미터의 메조포어(mesopore), 50 나노미터 이상의 매크로포어(macropore)로 분류된다. 본 연구에서는 다기능성 단량체를 합성한 후, 이를 다양한 반응으로 중합하여 높은 비표면적을 갖는 다공성 고분자를 합성하고 특성을 조사하였다.

아다만탄(Adamantane)에 아세틸렌기를 도입한 테트라키스(4-에티닐페닐)아다만탄과 벤젠-1,3,5-트라이싸이올의 싸이올-인(thiol-yne) 반응을 통하여 다공성 고분자를 제조하였다. Chloroauric acid의 환원 반응을 이용하여 금 나노입자를 고분자 내부에서 제조하고 고정화하였다. 제조된 금 나노입자가 면상입방구조를 갖는 것을 XRD로 확인하였다. 금나노입자가 도입된 다공성 고분자는 니트로페놀의 수소화반응에서 촉매활성을 보였다.

비스페놀-A와 4-브로모페닐이소시아네이트로부터 합성한 주형분자 복합체와 테트라키스(4-브로모페닐)메탄의 Yamamoto 반응을 이용하여

고분자를 제조한 후 주형분자를 제거하는 방법으로 비스페놀-A를 인식할 수 있는 다공성 고분자를 제조하였다.비스페놀-A가 날인된 다공성 고분자는 562 m^2/g의 비표면적을 나타냈으며 비스페놀-A에 대해서 우수한 인식능력을 보였다.

테트라페닐에텐을 빌딩블록으로 이용하여 다공성 고분자를 제조하였다. 테트라키스(4-요오드페닐)에텐과 1,4-디에티닐벤젠, 1,3,5-트리에티닐벤젠, 테트라키스(4-에티닐페닐)아다만탄의 소노가시라-하기하라(Sonogashira-Hagihara) 반응을 이용하여 400-1200 m^2/g의 비표면적을 갖는 다공성 고분자를 얻었다. 1,4-디에티닐벤젠과 1,3,5-트리에티닐벤젠의 몰 비 3:2 혼합물과 테트라키스(4-요오드페닐)에텐으로부터 합성한 다공성 고분자는 1800 m^2/g 이상의 비표면적을 보였다.

1,3,5-트리클로로벤젠 또는 1,3,5-트리(4-브로모페닐)벤젠과 디비닐벤젠의 Heck 반응을 이용하여 다공성 고분자를 제조하고, 이를 탄화시킨 후 기공성의 변화를 조사하였다. 탄화 후 1 나노미터 이하의 마이크로 기공이 증가하였으며, 수소 및 이산화탄소에 대한 흡착성능이 향상되었다.

주요어 :다공성 고분자, 금 나노입자, 가스저장, 촉매, 분자날인.

학번 : 2006-20875

List of Publication and Patents

(1) Hyunpyo Lee, Jun Bum Park and Ji Young Chang. **Synthesis of Poly(ethylene glycol)/Polypeptide/Poly(D,L-lactide) Copolymers and Their Nanoparticles.** *Journal of Polymer Science Part A: Polymer Chemistry* **2011**, *49*, 2859-2865.

(2) Hyunpyo Lee, Hyun Woo Park and Ji Young Chang. **Preparation of Microporous Polymers Consisting of Tetraphenylethene and Alkyne Units.** *Macromol. Res.* **2013**, accepted for publication.

(3) Yoon Sung Kwon, Byung Mun Jung, Hyunpyo Lee and Ji Young Chang. **Preparation of Polymeric SWNT-Liquid Crystal Composites Using a Polymerizable Surfactant** *Macromolecules*, **2010**, *43*, 5376-5381.

(4) 장지영, 이현표, 박준범 *폴리 (에틸렌 글리콜)-b-[폴리(L-세린)-g-폴리(D,L-락티드)] 의 블록공중합체 및 이를 이용한 약물전달체용 나노입자의 제조 방법*, 특허등록 제 10-0987693호.

List of Presentations

(1) 2008년 4월, 춘계 한국고분자학회, **PEG-PLLA-PDLLA을 이용한 암 공격용 층상 고분자 나노입자의 제조.**

(2) 2008년 10월, 추계 한국고분자학회, **Preparation of layered Polymer Nanoparticles from a PEG-PLLA-PDLLA Tri-block Copolymer.**

(3) 2009년 4월, 춘계 한국고분자학회, **Preparation of polymeric nanoparticles from a poly(ethylene glycol)-poly(phenylalanine)-poly(D,L-lactic acid)triblock copolymer.**

(4) 2009년 10월, 추계 한국고분자학회, **Polymeric nanoparticles obtained from a poly(ethylene glycol)-poly(phenyl alanine)-poly(D,L-lactic acid) Triblock copolymer.**

(5) 2009년 10월, The federation of asian polymer societies, **Polylactide grafted poly(ethylene glycol)-b-poly(L-serine) block copolymers and their nanoparticles.**

(6) 2010년 4월, 춘계 한국고분자학회, **Preparation of Polymeric Nanoparticles Bearing Europium(III) From Poly(glycolic acid-aminophenanethroline-aspartic acid)-co-Poly(L-lactic acid)**

(7) 2012년 4월, 춘계 한국고분자학회, **Preparation of Microporous Polymer Networks by Heck Cross-coupling Reaction.**